

Millimeter-Wave Seeing Inferred from Radiosonde Observations —
Preliminary Results

F. R. SCHWAB AND D. E. HOGG

August 31, 1988

1. Introduction. Weather balloons are launched twice daily (at 0h and 12h UT) from over one-hundred National Weather Service upper air observing stations and cooperating stations. At most of these places this program of observations has been in place continuously for the past 20–40 years. A few of the stations are located in the same geographical regions as potential MMA sites. The balloon flights provide, by means of radiosonde telemetry devices, profiles of the tropospheric temperature, relative humidity, and barometric pressure, as functions of altitude, for altitudes from ground level up to typically 20–30 km.¹

From these observations one can obtain, directly, an estimate of the water vapor density (i.e., the absolute humidity) at any given altitude (up to some moderate altitude where the humidity measuring device ceases functioning). One can integrate the water vapor density from some altitude upward, in order to obtain an estimate of the column density of water vapor. Taken together with a model for millimeter-wave propagation through moist air, such as Liebe's model (Liebe, 1985), one can estimate millimetric wavelength zenith opacities for any given site elevation.

The radiosonde data provide no direct information on clouds (i.e., neither their presence nor their composition), whose contributions to zenith opacity we nevertheless attempt to account for in Section 4.

We have obtained radiosonde data covering the period 1965–1984 from the general geographical regions of several potential MMA sites: namely, radiosonde data from Albuquerque NM, Tucson AZ, Winslow AZ, Denver CO, and Grand Junction CO. The results of preliminary analyses of these data are summarized below. We expect soon to obtain data from three additional sites: El Paso TX, Hilo HI, and Antofagasta Chile (located on the northern coast of that country).

2. Precipitable Water Vapor. Plots of precipitable water vapor vs. time, for the period 1965–1984, are shown in Figures 1–6. The ordinate of each plot is precipitable H₂O vapor (PWV), measured in units of grams per square centimeter (1 g/cm² column density of H₂O vapor equals 10 mm PWV). The location of the weather station is noted at the top of each plot, alongside the base altitude used in the integration. Two plots are shown for Albuquerque: one using a base altitude for the integrations of 7000 ft (the elevation of the VLA site), and one a base altitude of 10,500 ft (the approximate elevation of South Baldy). Spatial correlation over the western and southwestern U.S. is evident in these data, as similar year-to-year trends are evident in these plots. Some years appear to be very much better (i.e., drier) than others; 1971 and 1972, for example, tend to be better than the other years shown.

These data (all points ≤ 25 mm H₂O) are again displayed in Figures 7–12. In each of these plots, typically forty data points are shown for each day of the year—two launches

¹Wind speed and direction, obtained by means of radio direction finding, are also reported; for this reason the observations are technically referred to as *rawinsonde* observations, rather than *radiosonde* observations.

per day over a twenty year period; altogether there are approximately 14,600 data points in each plot.

Daily medians for each site are shown in Figures 13–18. That is, for any given day of the year (Feb. 29 excepted) the ordinate value is the median of the (typically forty) values obtained for that day of the year.

Figure 19 is a scatterplot of Winslow PWV vs. Tucson PWV, with a 45° line penciled in. We made a day vs. night comparison for just one site (Albuquerque), where we found slight differences that may merit further attention.

3. 225 GHz Opacities. Harry Lehto, a University of Virginia astronomy graduate student working at the NRAO in Charlottesville, has, during the course of his thesis work involving VLA data, written a Fortran program implementing Liebe's (1985) millimeter-wave propagation model. We have used a modified version of his code in our work. Liebe's model incorporates empirically derived spectroscopic parameters, over 450 in number, describing on the order of one-hundred O₂ and H₂O absorption lines; this model also includes empirically determined continuum spectra for dry air, water vapor, and hydrosols.

Plots of the median 225 GHz opacities for each of the sites, ignoring cloud effects, are shown Figures 20–25. The plots for Albuquerque, Tucson, and Winslow are qualitatively similar, as are the Denver and Grand Junction plots. All areas, if adjusted for altitude differences, might appear to be about equally good in winter. The desert sites appear to be worse in midsummer than the Colorado sites. On the left of the summer peaks in the Colorado plots are gentle 'wings' (also evident in the PWV plots), suggesting that conditions in Colorado tend to deteriorate earlier on in the springtime than is the case in the desert areas of New Mexico and Arizona.

A scatterplot of estimated 225 GHz opacities vs. PWV for one site, Tucson, is shown in Figure 26. In Figure 27 we show a smooth curve fitted to the data of Figure 26, together with a sketched-in straight line relationship,

$$\tau_{225} = 0.005 + 0.056 \text{ PWV}_{(\text{mm})}, \quad (1)$$

that was assumed valid in MMA Memorandum No. 45; interestingly, the upper envelope of the data very nearly coincides with this straight line. The curve shown in Figure 27 is approximately linear for $\text{PWV} > 6$ mm, and in that regime its *slope* is close to the value of ~ 0.056 nepers per millimeter of PWV given by Zammit and Ade (1981) (evidently the source for Eq. 1). We are not certain how to reconcile our result with the paper of Zammit and Ade. The PWV data shown in their paper do not include any points lower than about 5 mm PWV.

A scatterplot of estimated 345 GHz opacities vs. 225 GHz opacities for Tucson is shown in Figure 28. The relationship appears to be slightly curvilinear, with slope ≈ 3.6 or 3.7 at the origin, decreasing to ~ 3.3 at the right-hand side of the plot.

4. Opacities, Including the Effects of Clouds. The radiosonde data provide no direct information on clouds; this is unfortunate because thick, liquid hydrosol laden clouds severely affect millimeter-wave seeing. A simple-minded approach for inferring the presence of clouds is to assume that a cloud is present wherever the relative humidity is high; then one must make a guess about the density of liquid water within the cloud. This approach, which we have adopted, was used earlier in work by Decker *et al.* (1978).

We have adopted the following cloud model: We assume that a cloud is present in the neighborhood of any relative humidity reading in excess of 95%. We take the height of

the bottom of the cloud to be the altitude (obtained by inverse interpolation) where the humidity first exceeds 94%, and we take the top of the cloud to be at the point where the relative humidity decreases to 94%. We assume a liquid density of 0.2 g/m^3 for clouds thinner than 120 meters and a density of 0.4 g/m^3 for clouds thicker than 500 meters; for clouds in the intermediate thickness range, we linearly interpolate according to thickness. This cloud model is intermediate between cloud models 2 and 3 of Decker *et al.* We use the hydrosol continuum model of Liebe's (1985) Section 2.3 in order to estimate the cloud contribution to opacity.

Thus far, we have analyzed only the Denver data in this manner. 'Clouds' were found to be present in 3803 of the 14,575 launches, or 26.1% of the time. The results are summarized in Figures 29 and 30. Comparing Figure 30 with Figure 24, we see that, in this case, the median opacity estimates are little affected by inclusion of cloud effects.

5. Comparison of the Albuquerque Data with Data from the VLA and S. Baldy Tipping Radiometers. To date, our only comparison of radiosonde data with tipping radiometer data has been to compare the Albuquerque 10,500 ft altitude results with monthly medians of the South Baldy 225 GHz radiometer data, taken from MMA Memorandum No. 45. In Figure 31 the South Baldy data points, seventeen in all, are drawn as crosses superimposed upon the monthly median plot of the radiosonde data; the radiometer data points cover the period November 1986 through March 1988.

We have not yet made any comparisons of the radiosonde data with tipping radiometer data obtained at the VLA site. We plan to make more detailed comparisons with South Baldy and VLA data once we receive Albuquerque radiosonde data for the years 1986–1988.

6. Plans for Further Work. Our top priority is to obtain Albuquerque radiosonde data for the period 1985–onward and compare it with simultaneous data recorded by the VLA and the South Baldy tipping radiometers.² Our crude comparison of monthly medians of data from the South Baldy radiometer with daily medians, over an earlier 20-year period, of the Albuquerque radiosonde data showed good agreement. However, we would be much more strongly encouraged if, besides good mean seasonal agreement, we were to find strong correlation between radiosonde data and radiometer data obtained over the very same time periods.

We are soon to obtain radiosonde data covering the period 1965–1984 from El Paso, Hilo, and Antofagasta, which we plan to analyze in the same manner as we have done for the other weather stations. We plan to re-analyze the data from Albuquerque, Grand Junction, Tucson, and Winslow, this time including in the opacity estimates the effects of clouds, as in Section 4 above.

We will undoubtedly produce further summary plots of the data, including site vs. site correlations, 345 GHz opacity estimates, percentage of time opacity is less than a given value, etc.

As the list of potential MMA sites is narrowed, we may wish to re-do the radiosonde reductions, beginning the integrations at heights other than those chosen for our preliminary studies of the data (i.e., starting the integrations at the elevations of specific sites). When tipping radiometer data are obtained from other potential MMA sites besides the VLA and

²Albuquerque data through May 1988, which have already been ordered from the National Climatic Data Center, should be in hand by the time of the next MMA site/configuration group meeting, scheduled for September 8.

South Baldy we will, of course, want to compare those data with the opacities inferred from radiosonde observations.

Calculation of precipitable water vapor, 225 GHz opacity, and 345 GHz opacity for twenty years of data from a single station requires about 180 minutes of Convex CPU time; this corresponds, roughly, to an overnight run if the Convex is moderately loaded.

Acknowledgments. We thank Robert Martin and Paul Hackett, both of Steward Observatory, for providing us with copies of the radiosonde data that they have procured for their own site studies. We also thank Harry Lehto for furnishing us with his computer program implementing Liebe's millimeter-wave propagation model.

REFERENCES

- Decker, M. T., E. R. Westwater, and F. O. Guiraud (1978), "Experimental evaluation of ground-based microwave radiometric sensing of atmospheric temperature and water vapor profiles", *J. Appl. Meteor.*, **17**, 1788-1795.
- Hogg, D., F. Owen, and M. McKinnon, "First results from the site testing program of the millimeter-wave array", MMA Memorandum No. 45, February 1988.
- Lehto, H., *Ph. D. Thesis*, in preparation.
- Liebe, H. J. (1985), "An updated model for millimeter wave propagation in moist air", *Radio Science*, **20**, 1069-1089.
- Zammit, C. C. and P. A. R. Ade (1981), "Zenith opacity attenuation measurement at millimetre and sub-millimetre wavelengths", *Nature*, **293**, 550-552.

Water Vapor - 20 yr (Albuq. , 7000 ft)

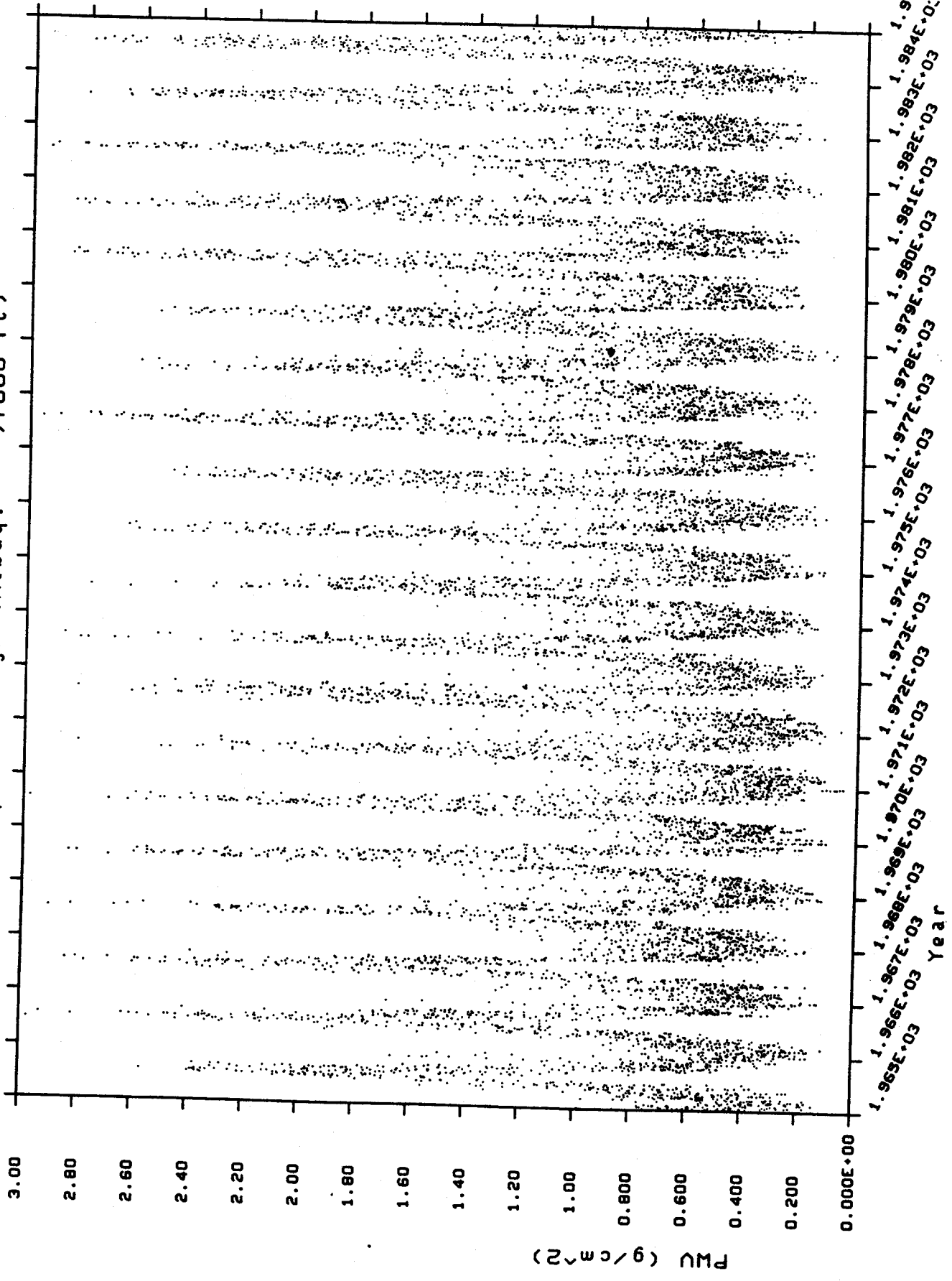


Fig. 1

Water Vapor - 20 yr (Albuq. ,10500ft)

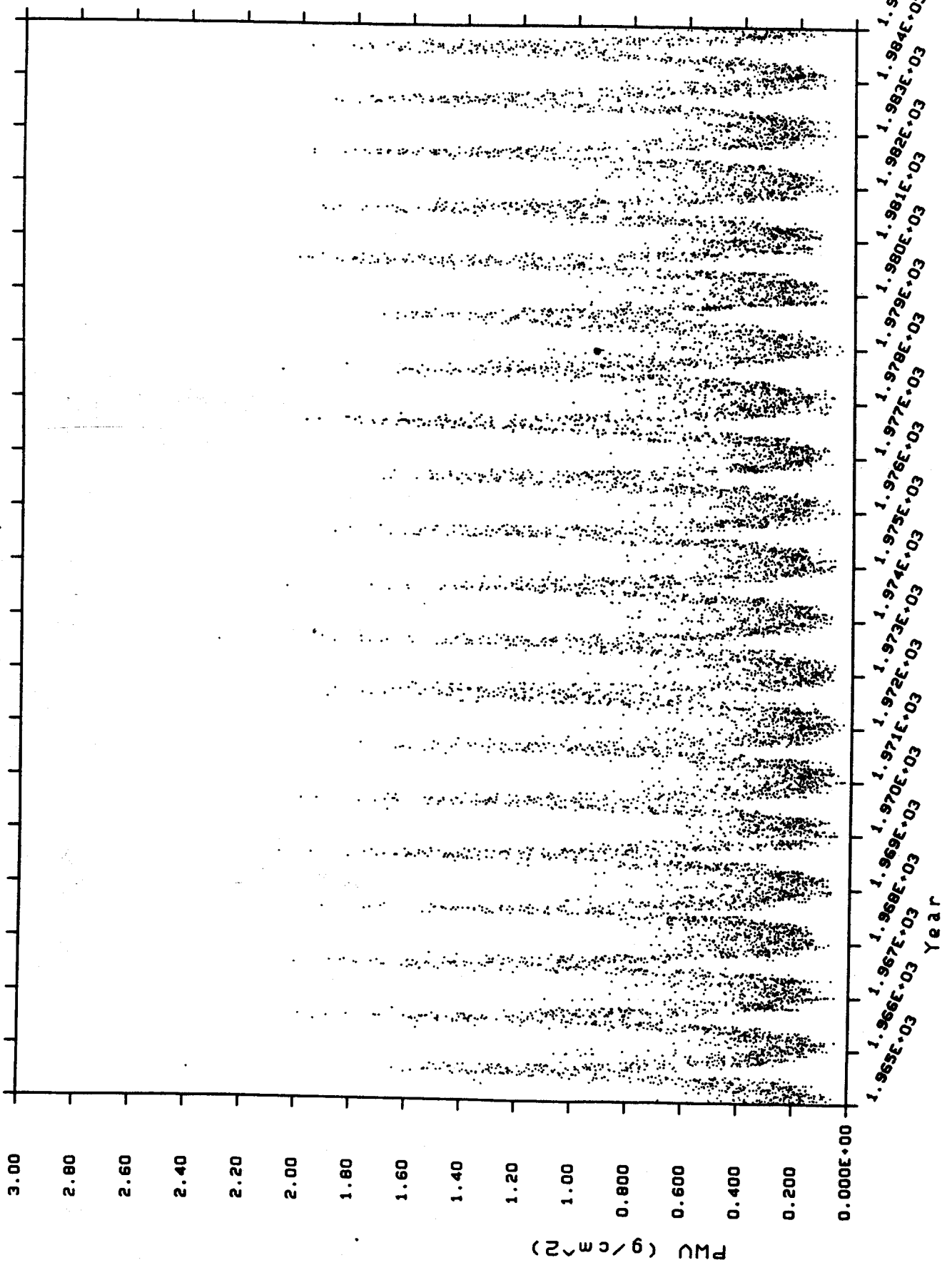


Fig. 2

Water Vapor - 20 yr (Tucson ,9300 ft)

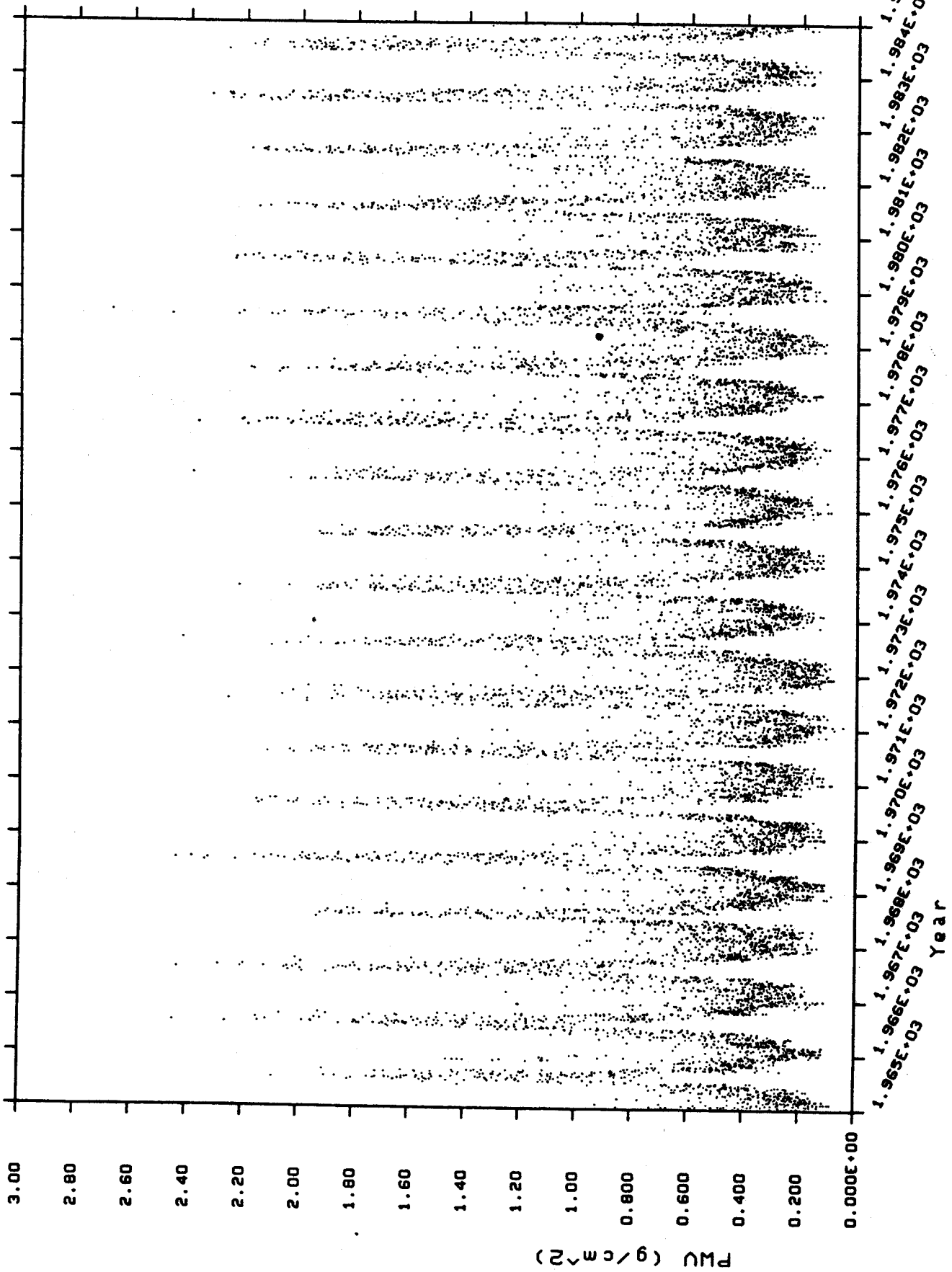


Fig. 3

Water Vapor - 20 yr (Winslow, 9300 ft)

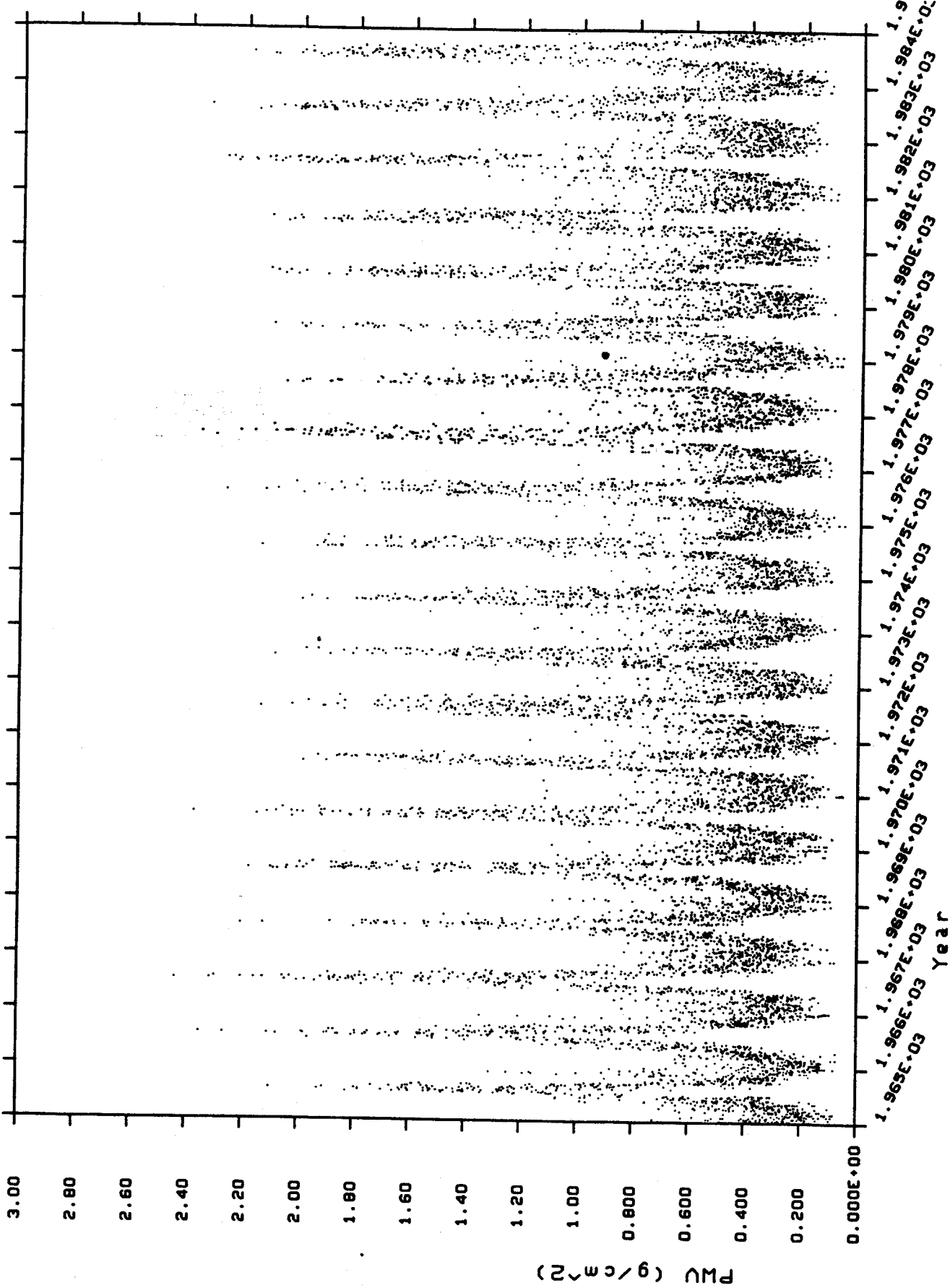


Fig. 4

Water Vapor - 20 yr (Denver ,9500 ft)

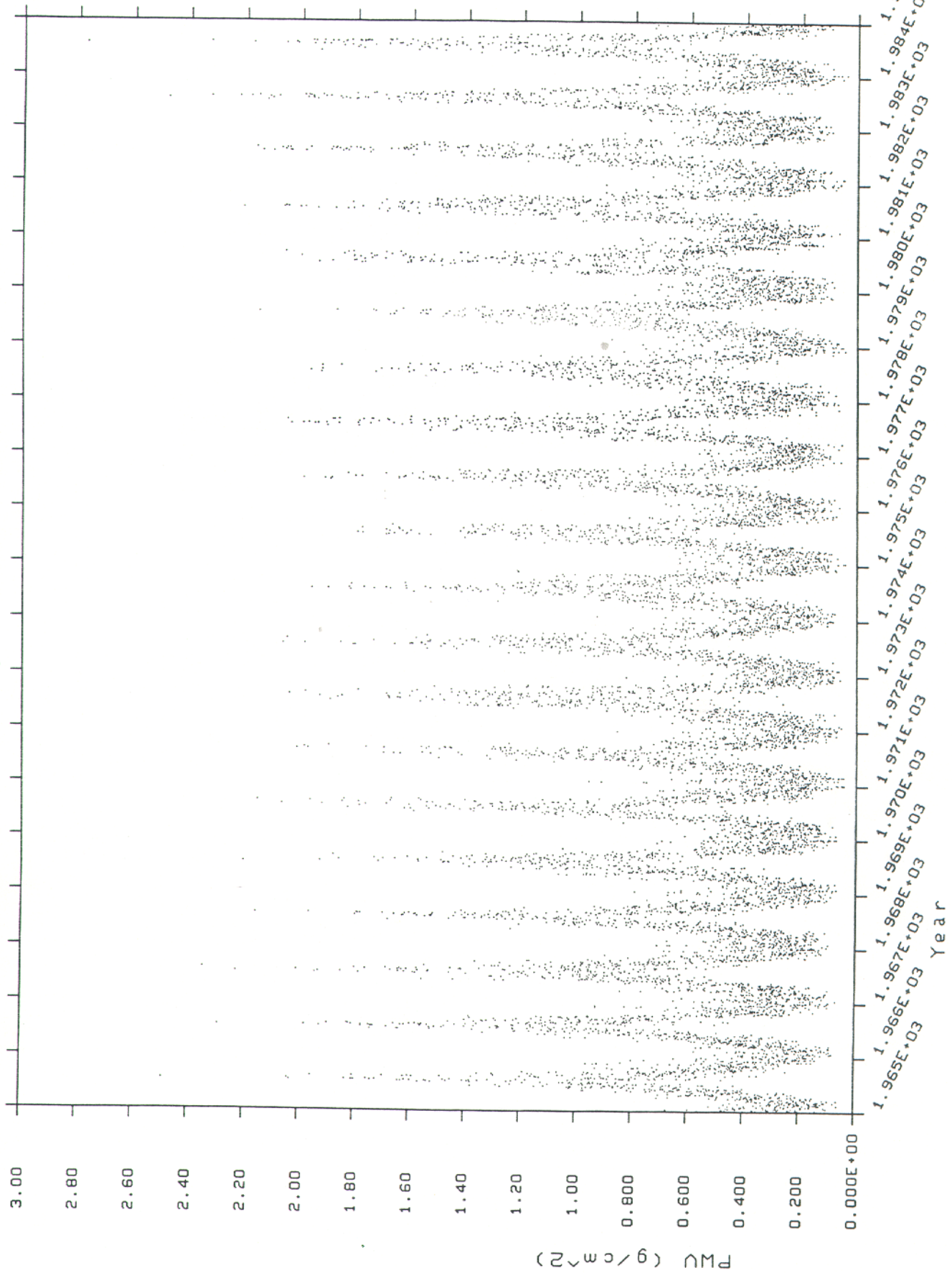


Fig. 5

Water Vapor - 20 yr (Gr. Jct. ,10000ft)

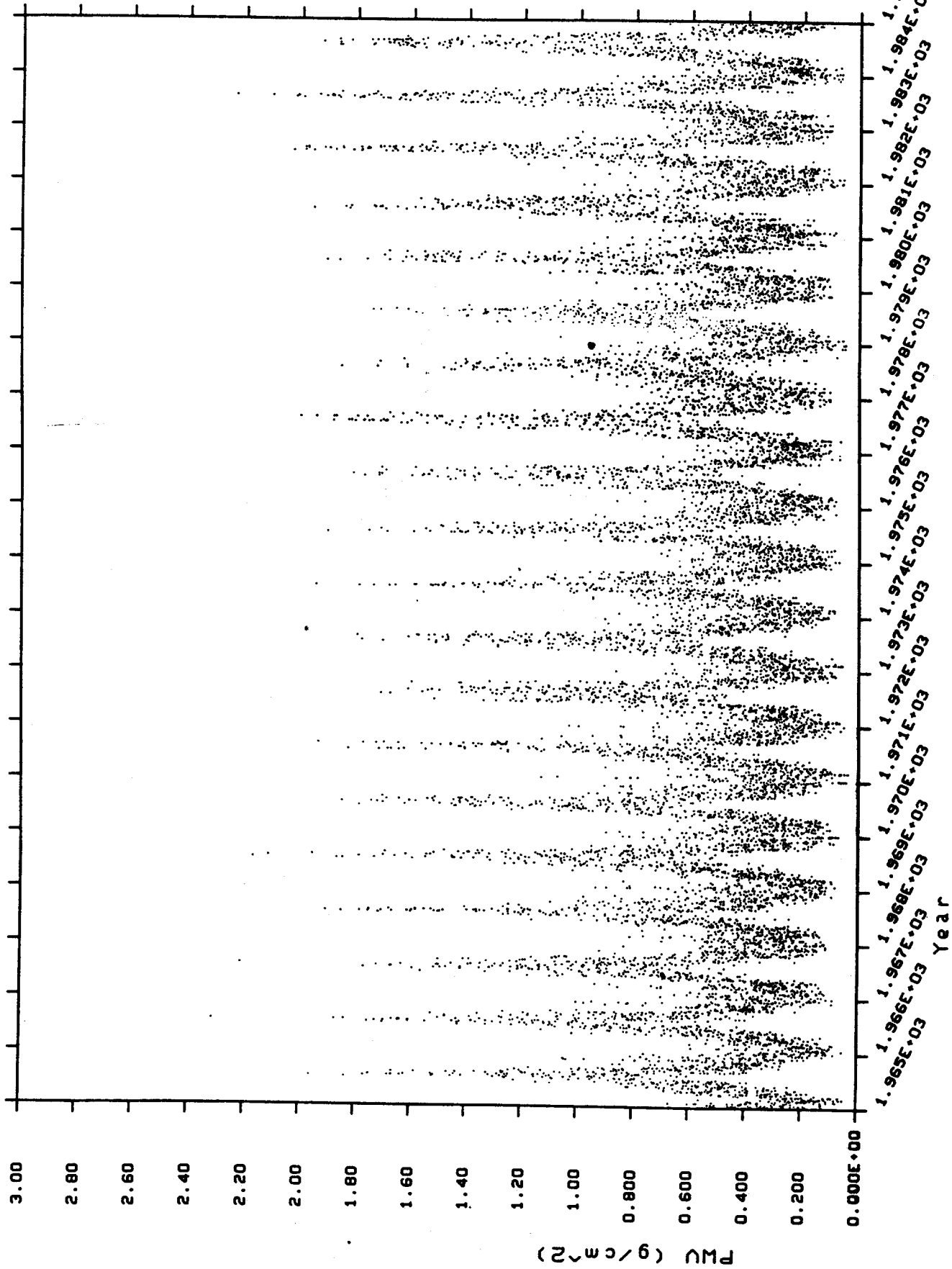


Fig. 6

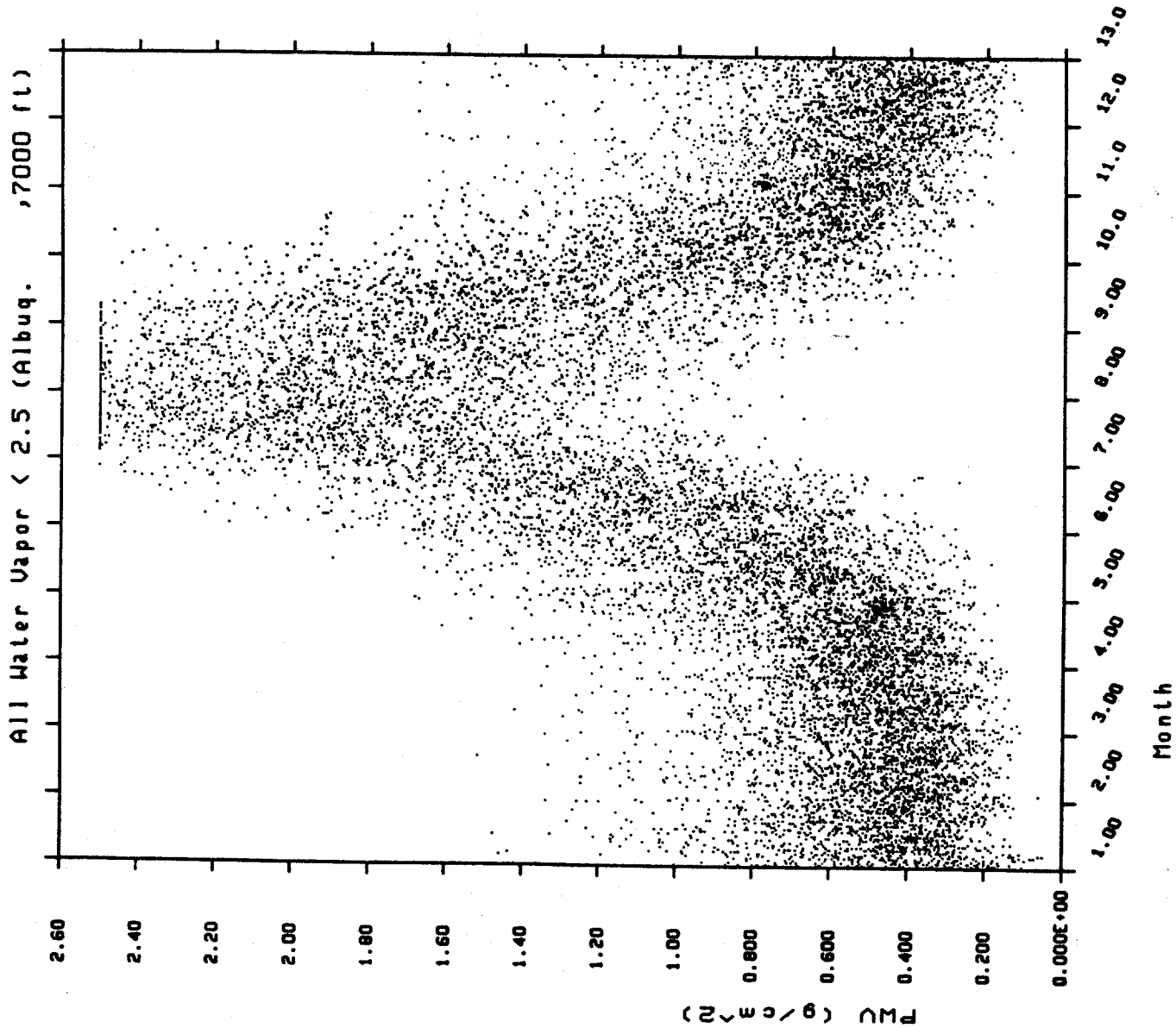


Fig. 7

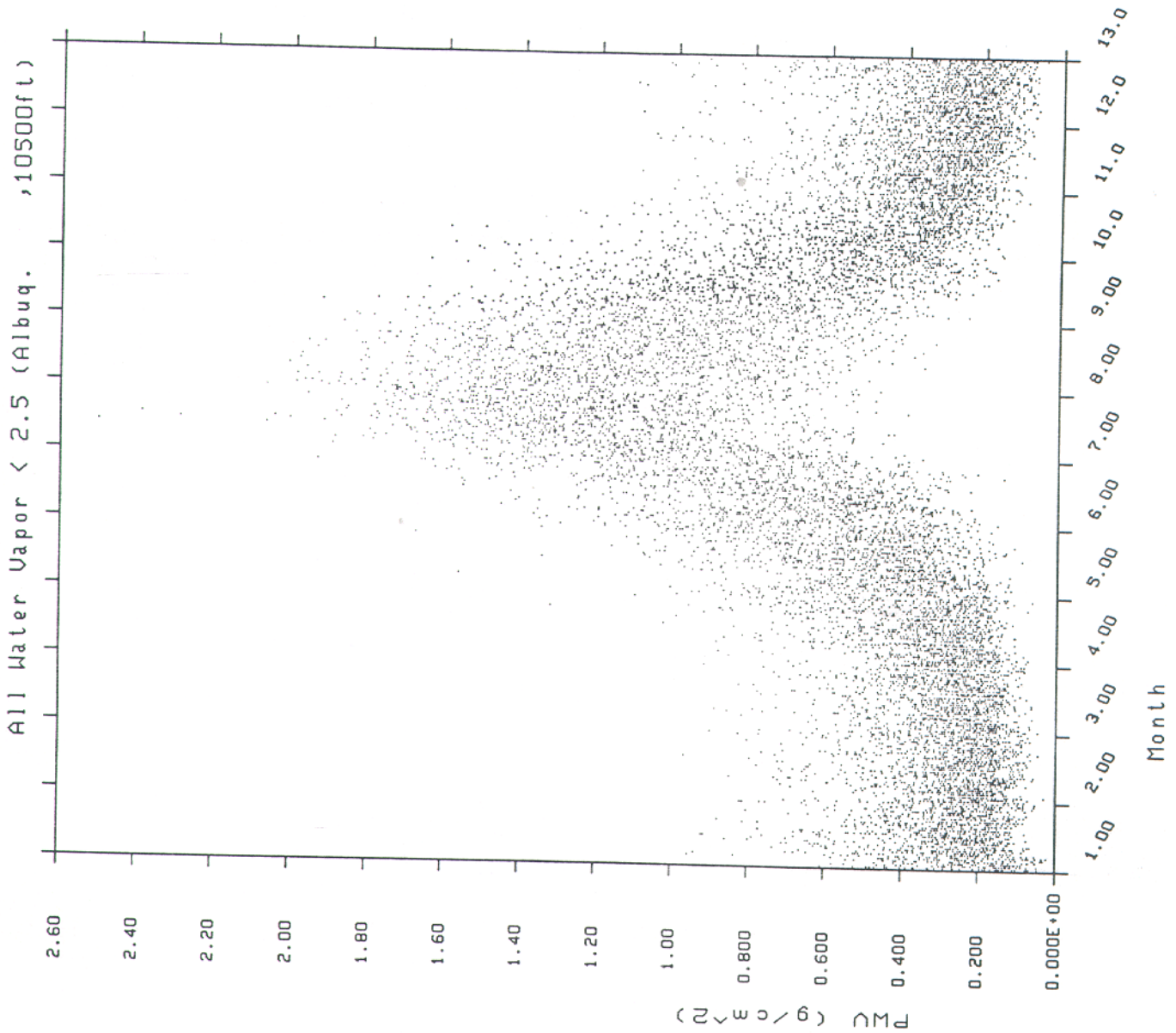


Fig. 8

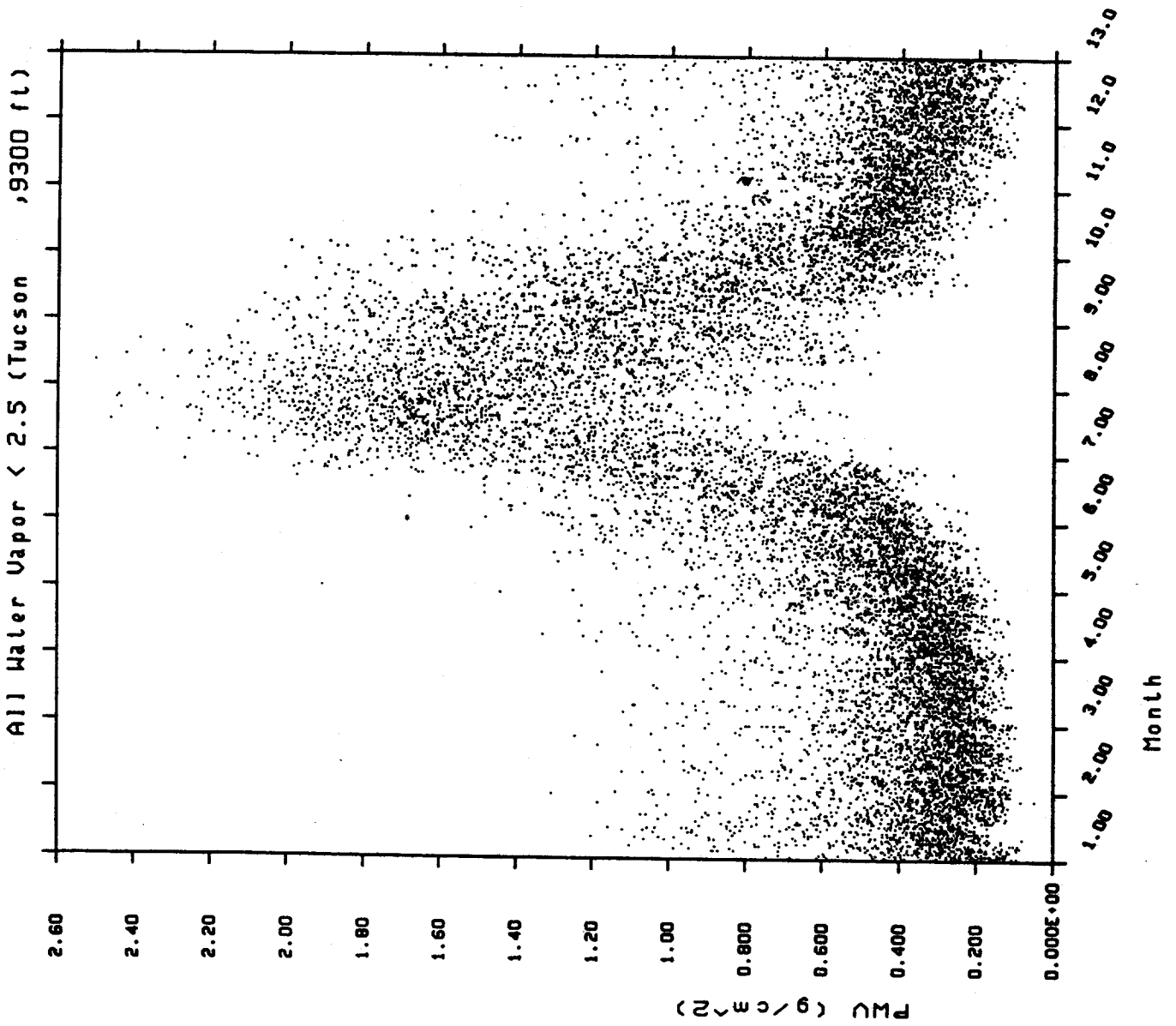


Fig. 9

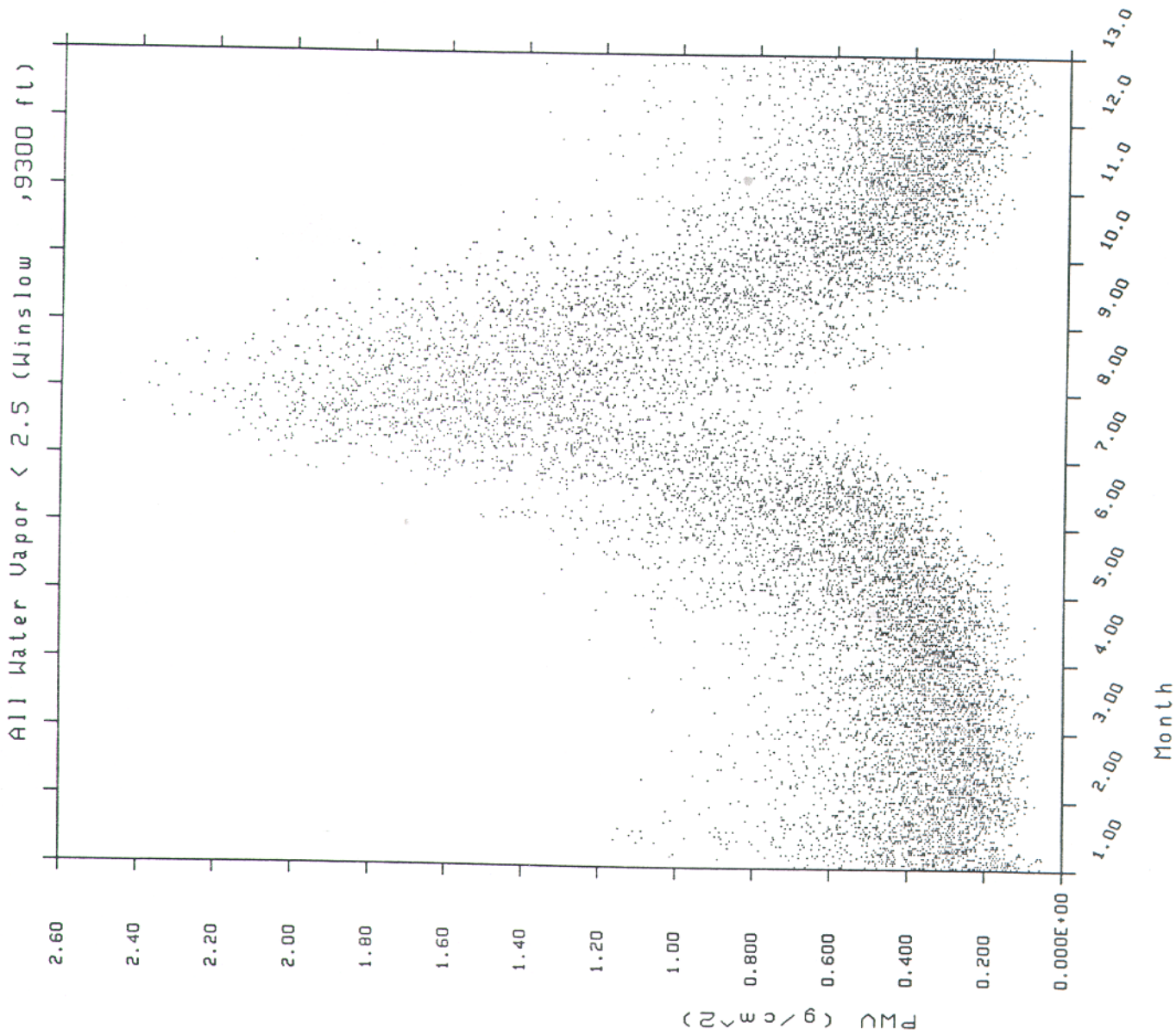


Fig. 10

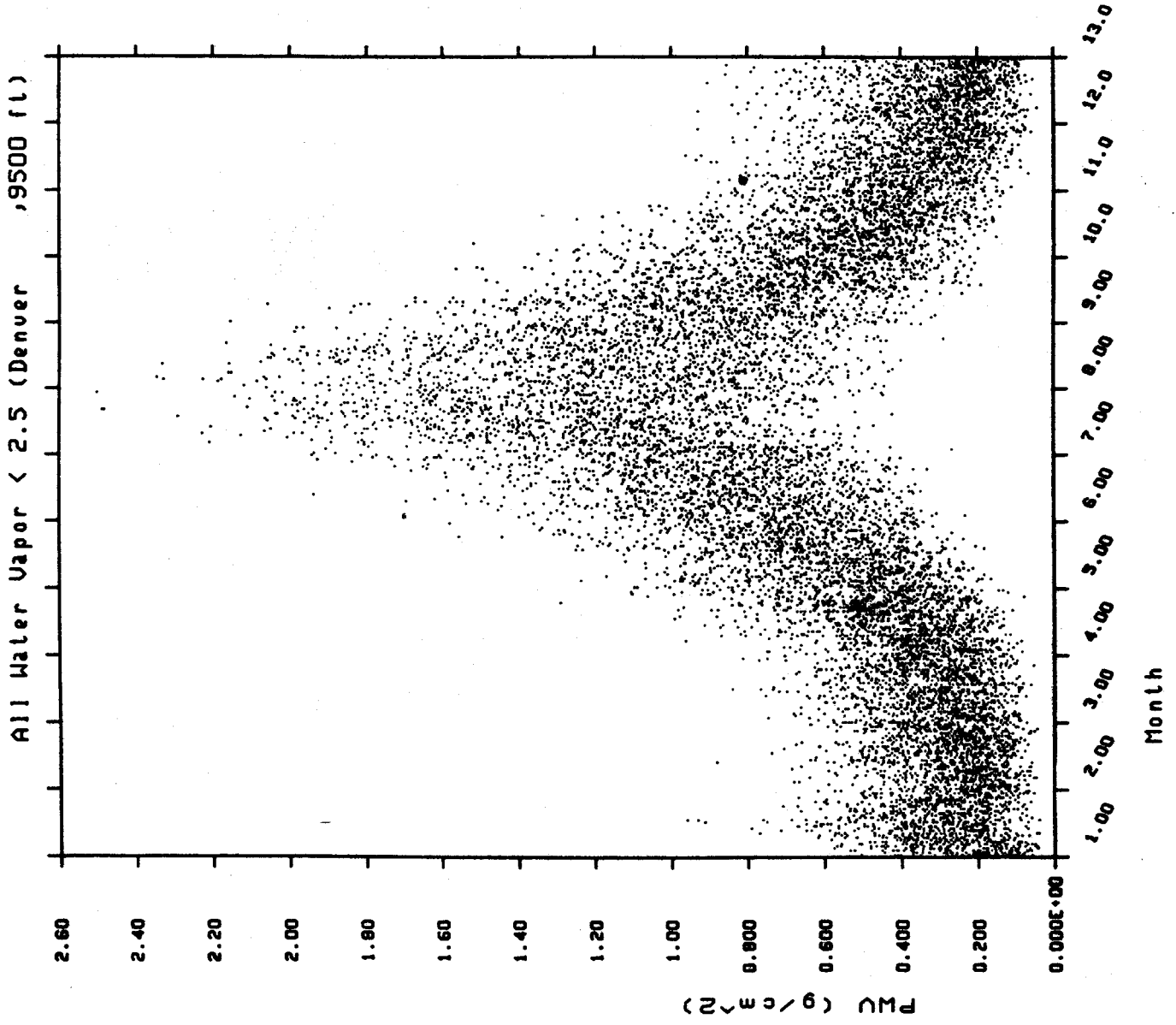


Fig. 11

All Water Vapor < 2.5 (Gr. Jct. ,10000ft)

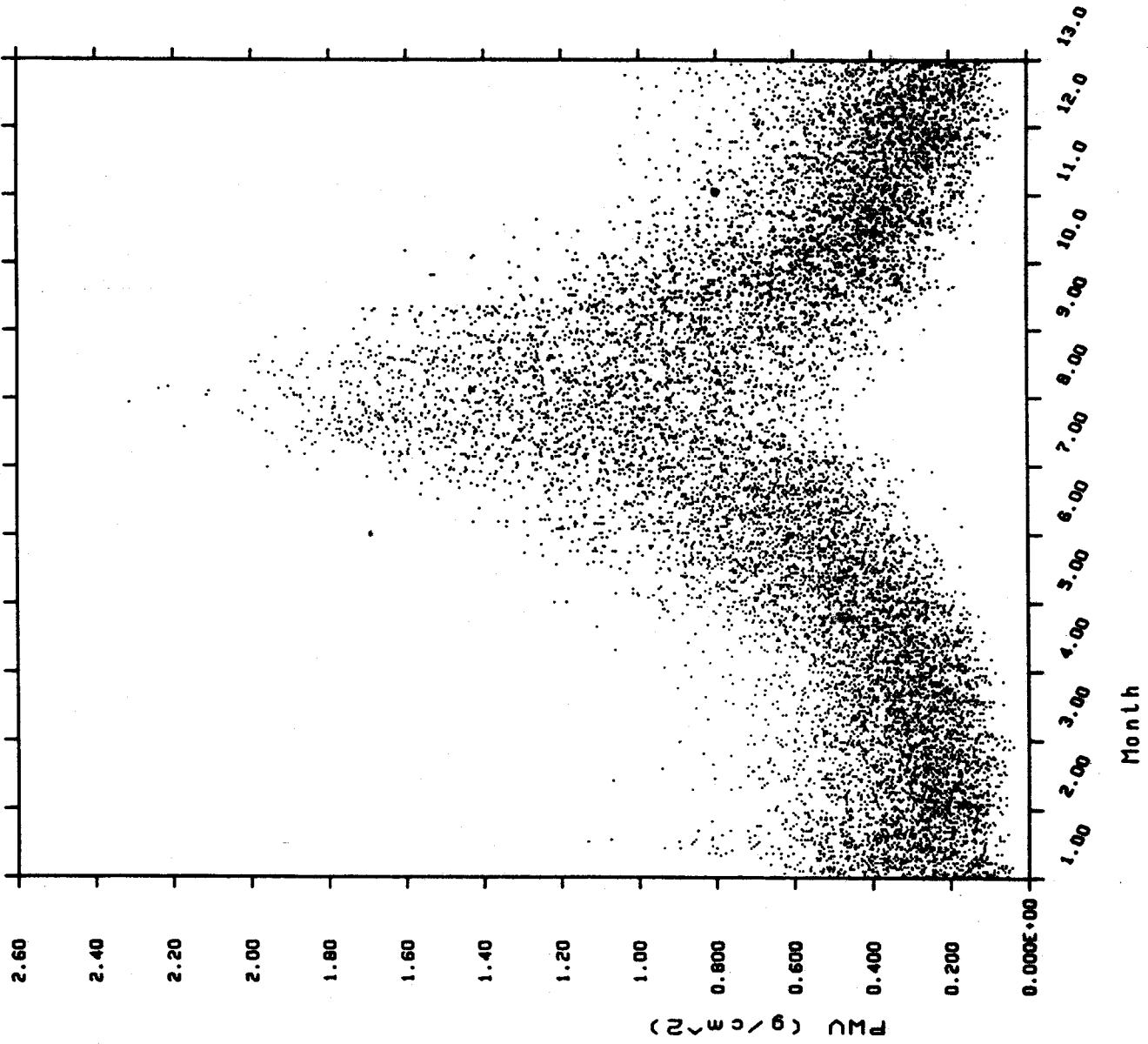


Fig. 12

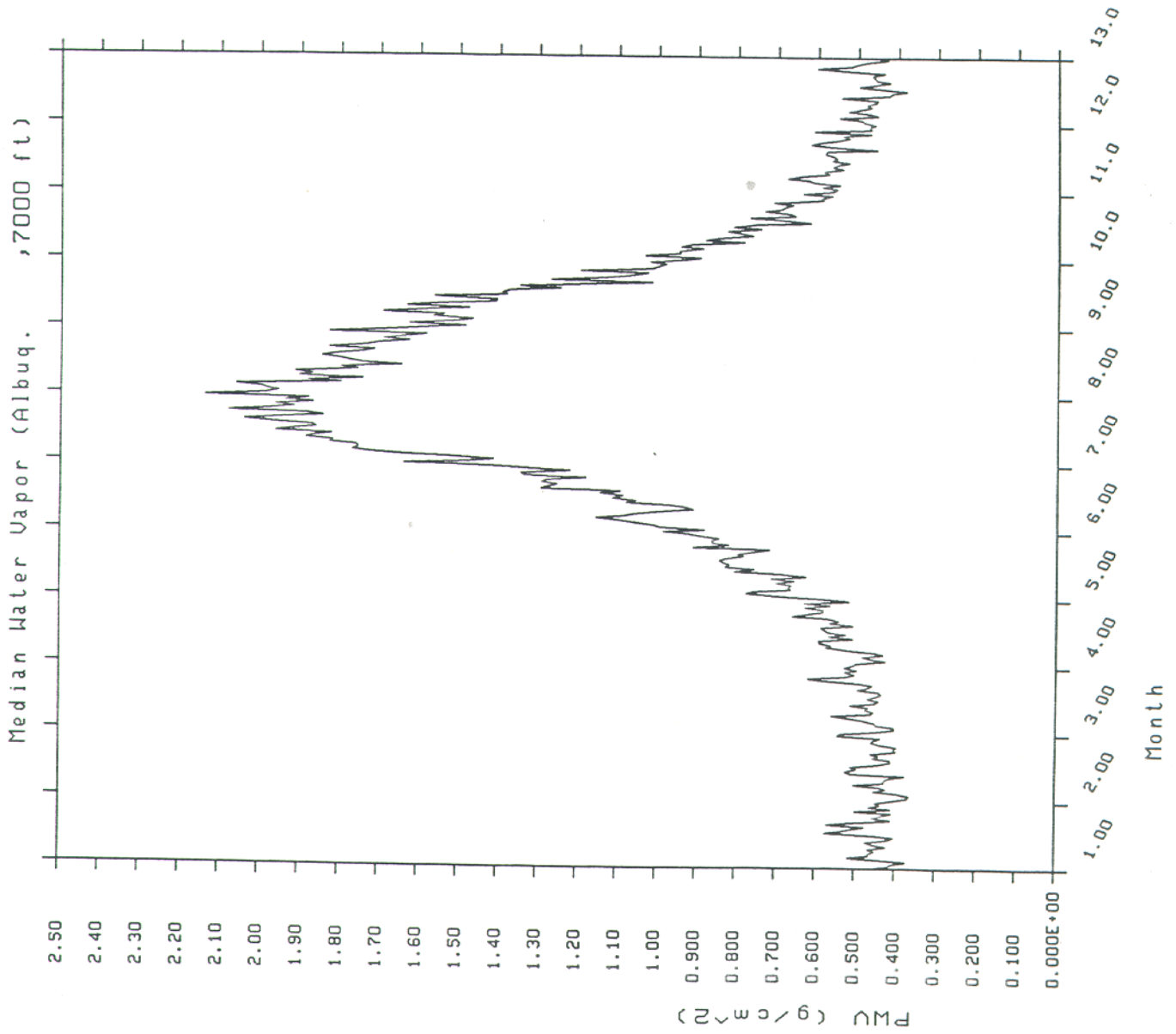


Fig. 13

Median Water Vapor (Albuq. ,10500ft)

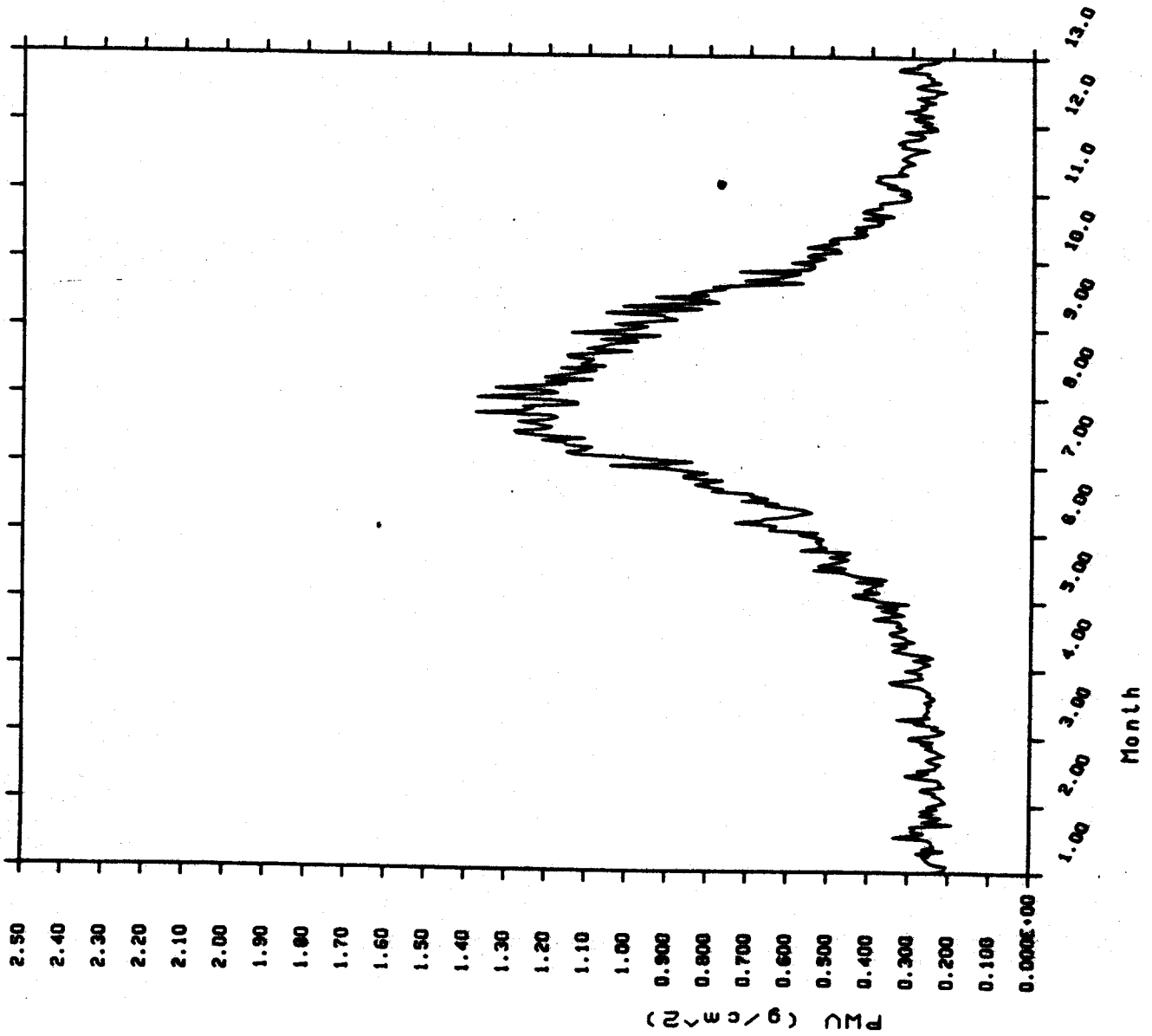


Fig. 14

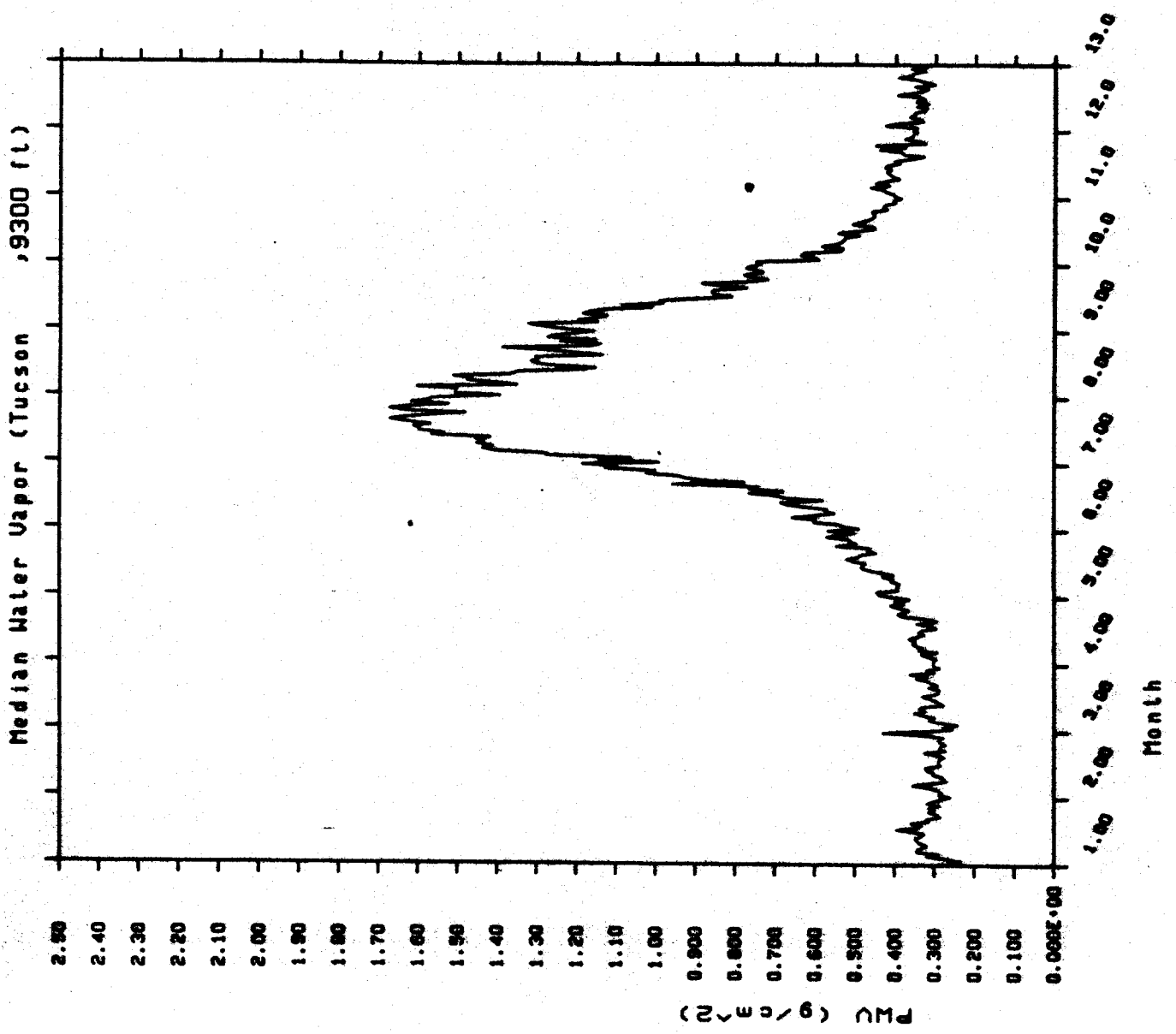


Fig. 15

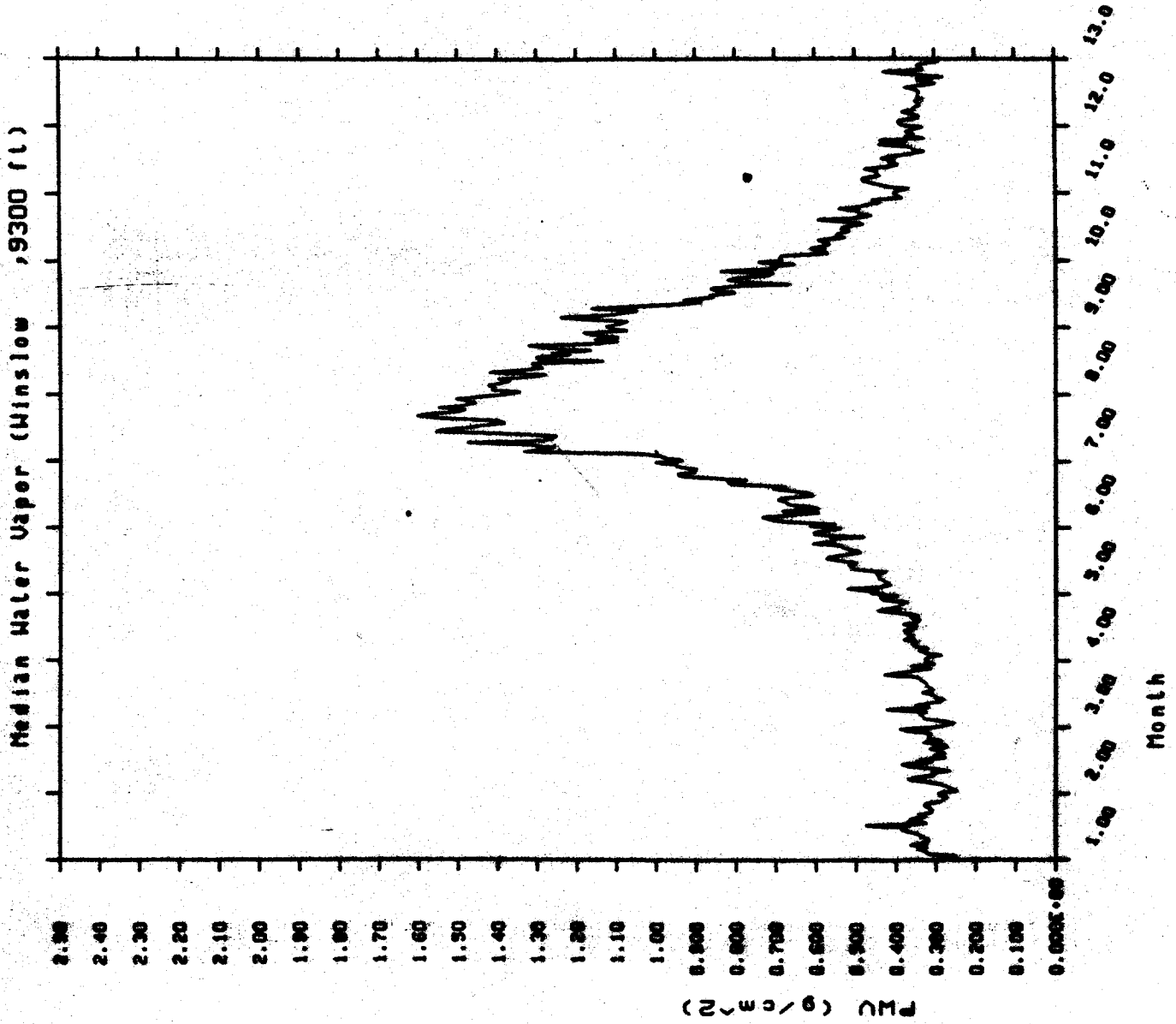


Fig. 16

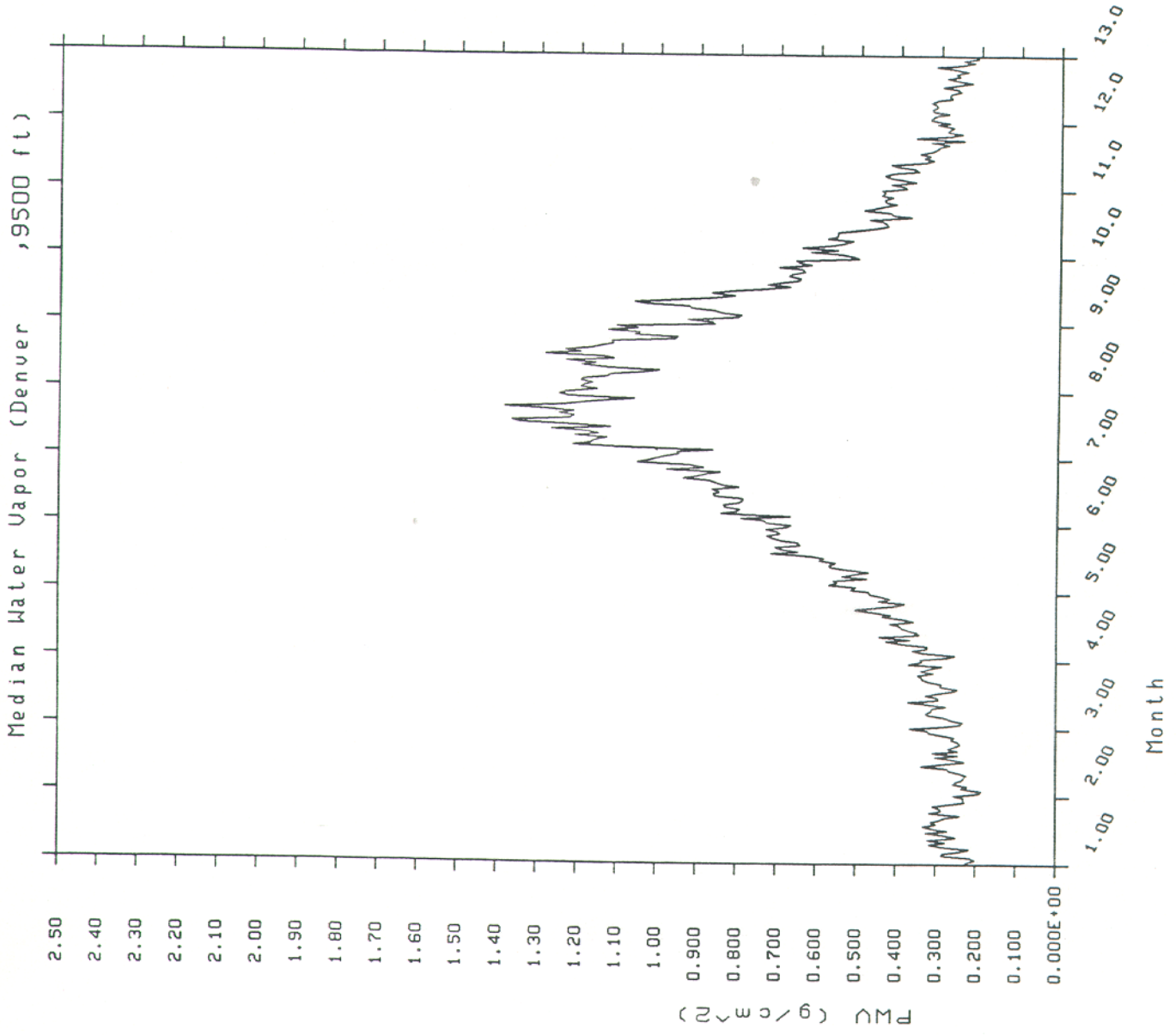


Fig. 17

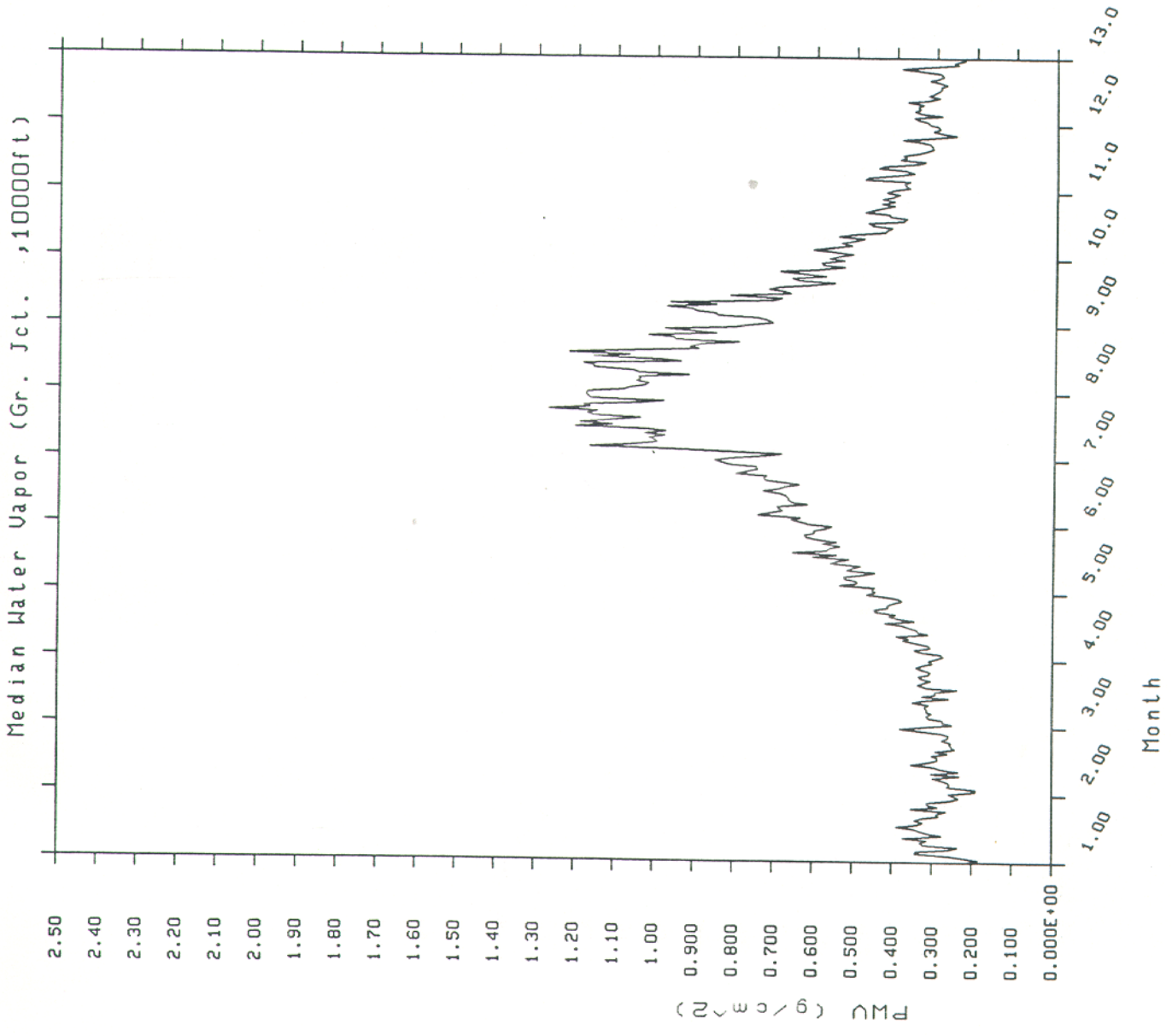


Fig. 18

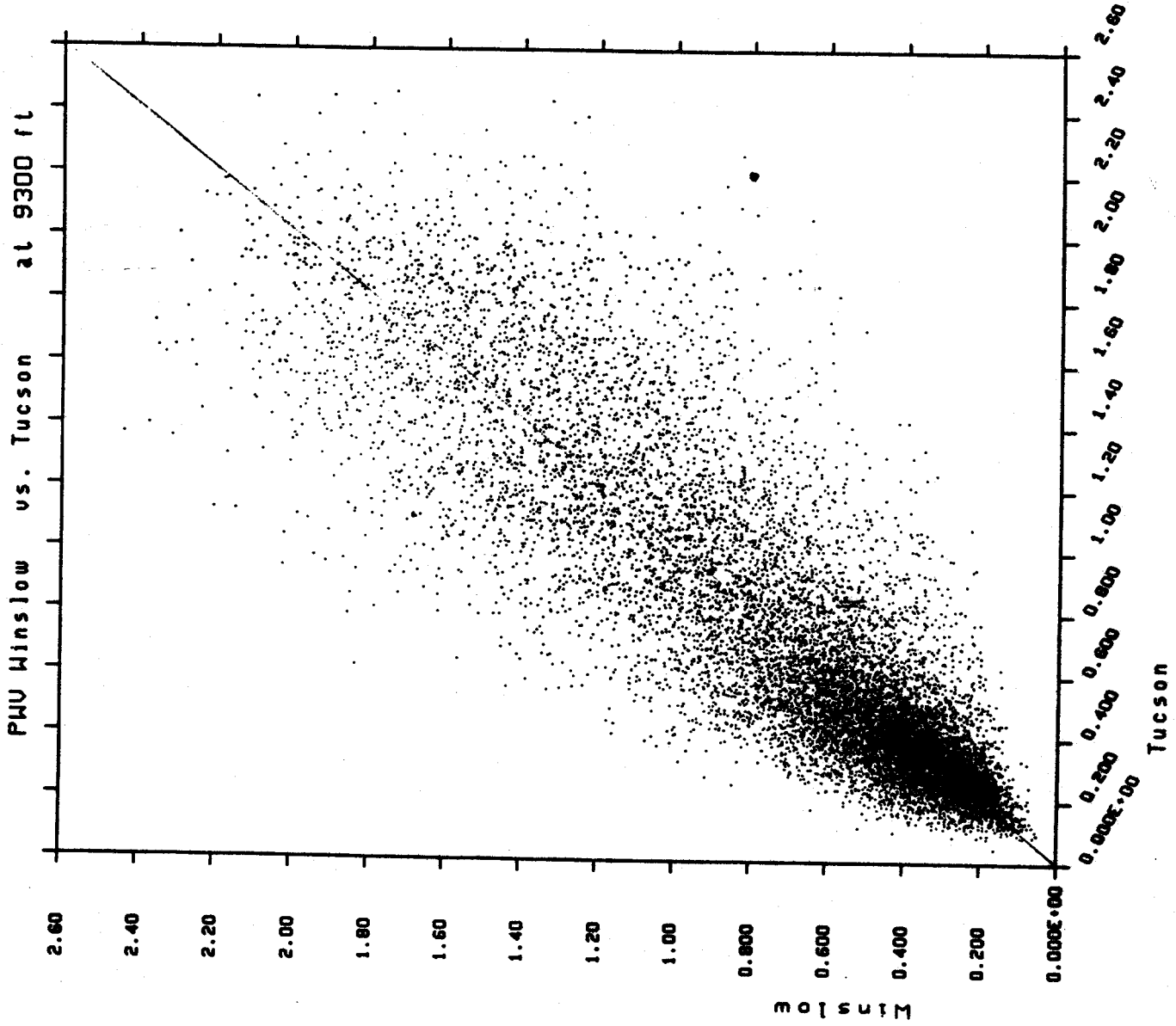


Fig. 19

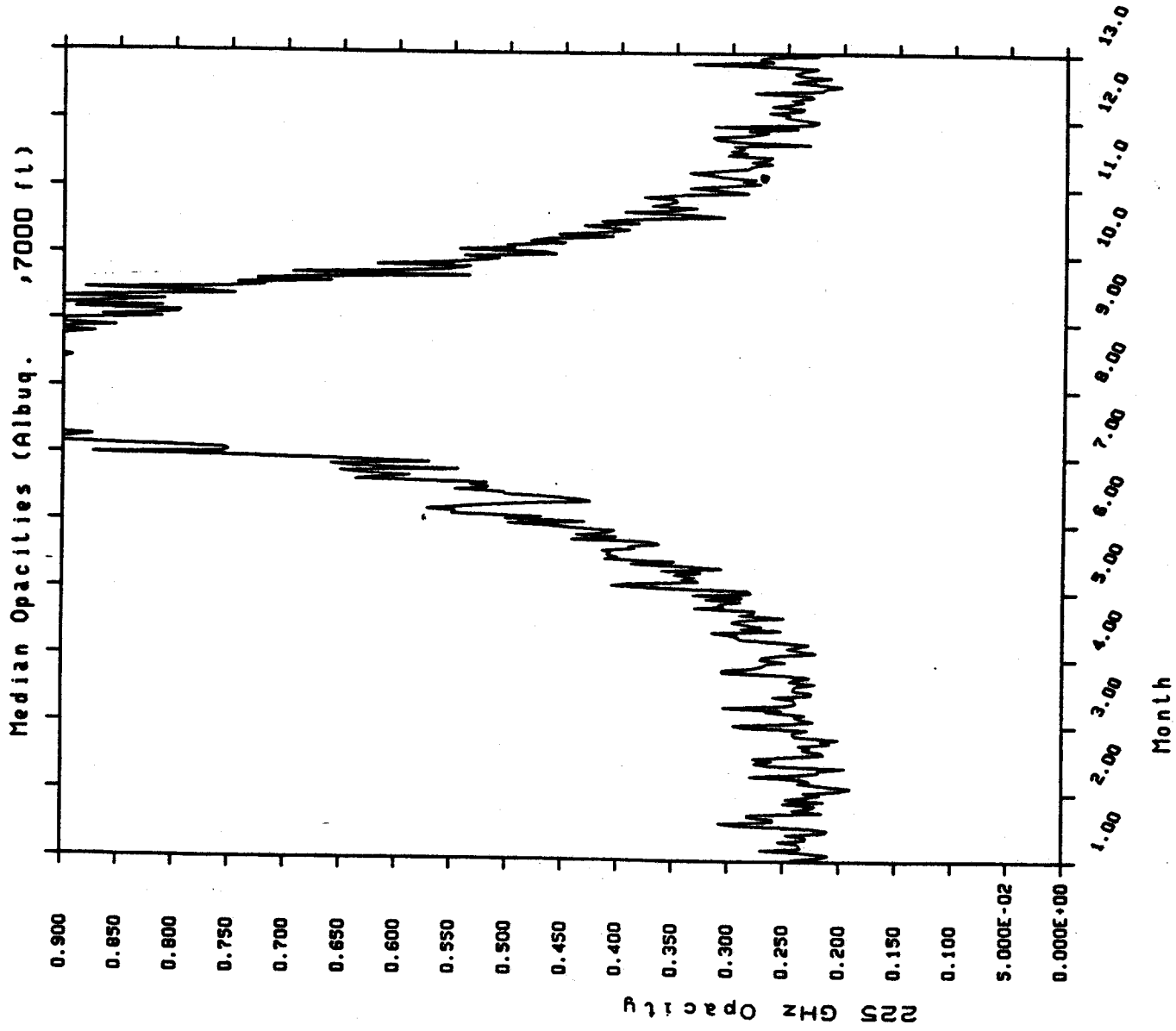


Fig. 20

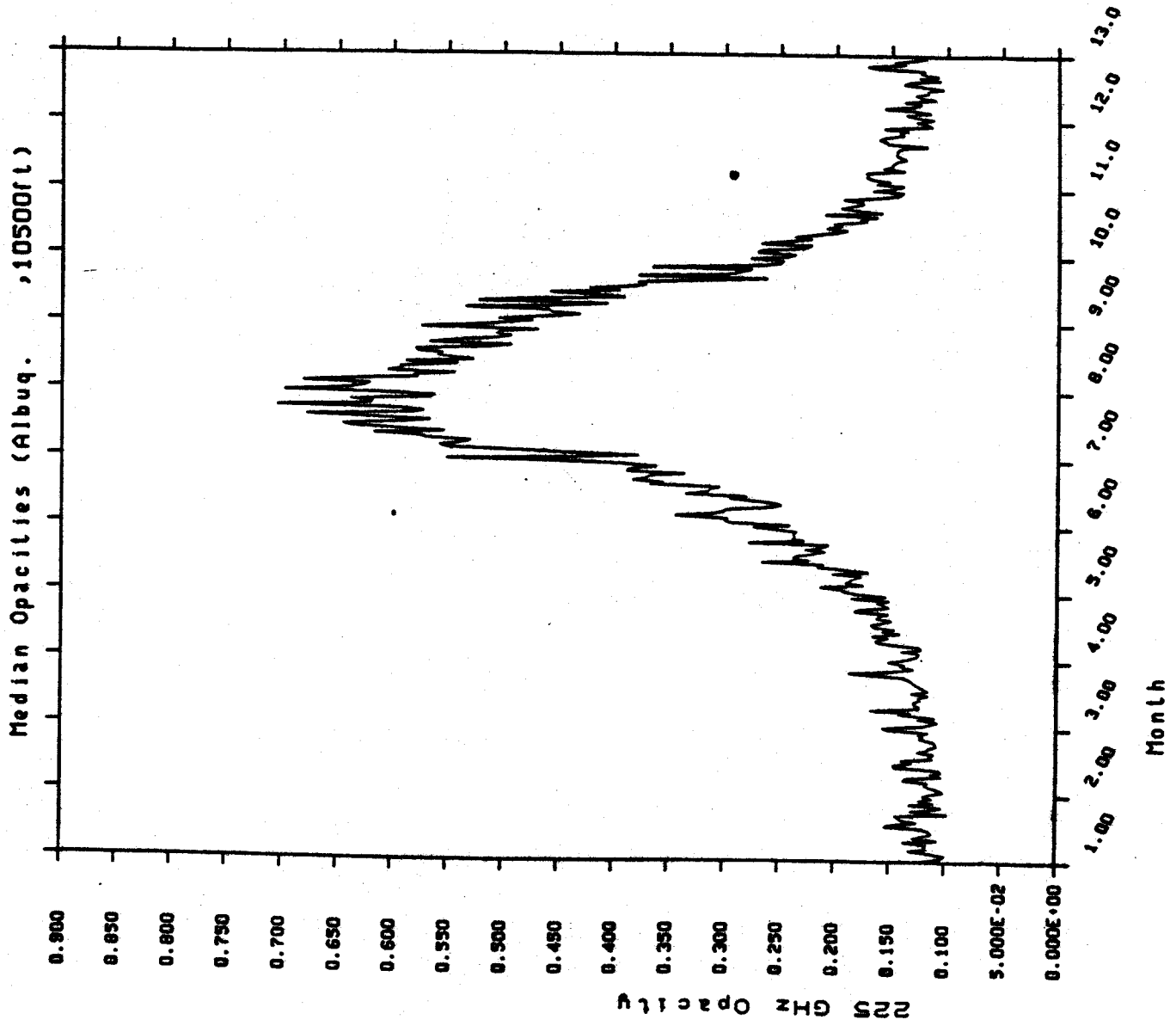


Fig. 21

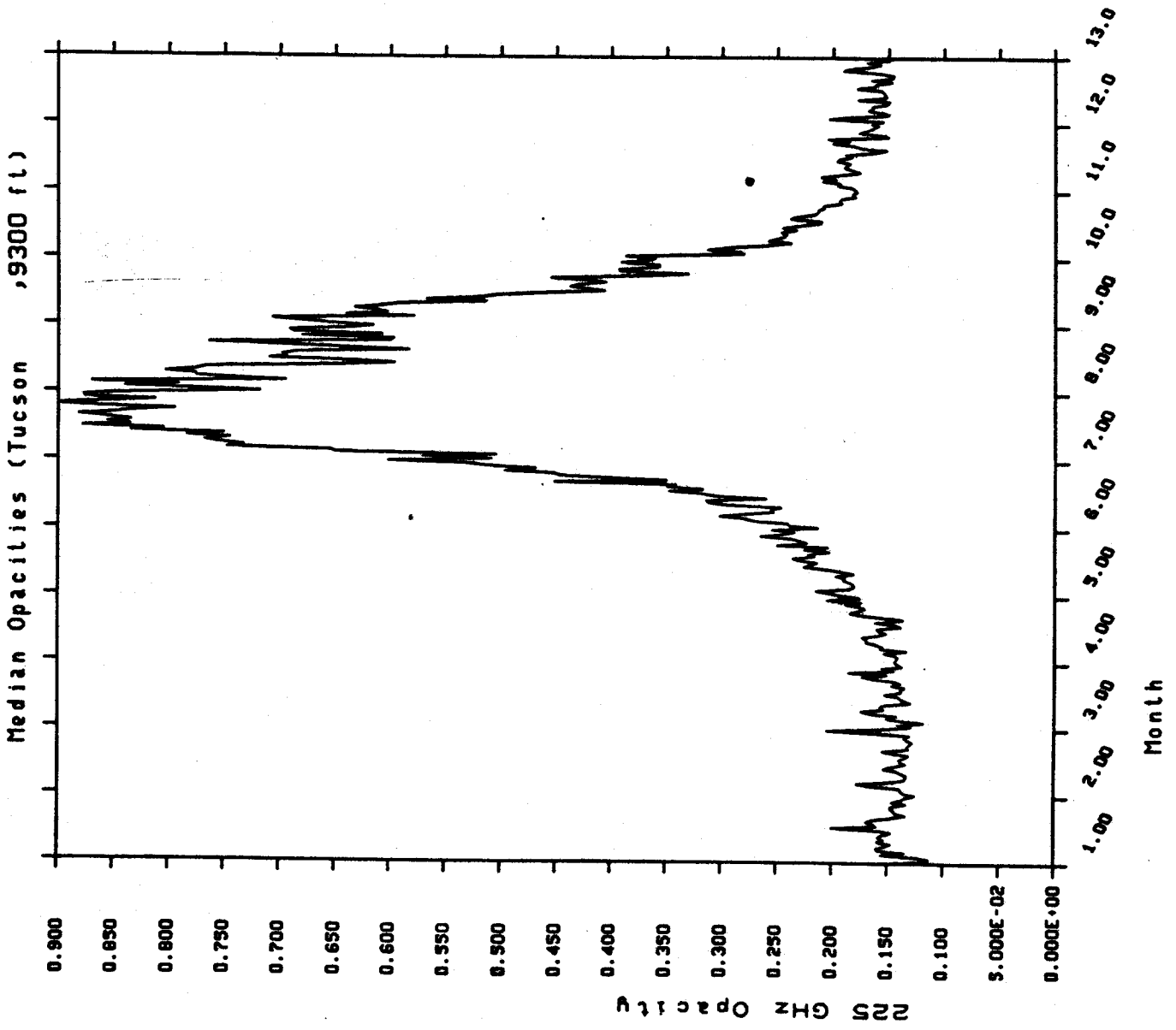


Fig. 22

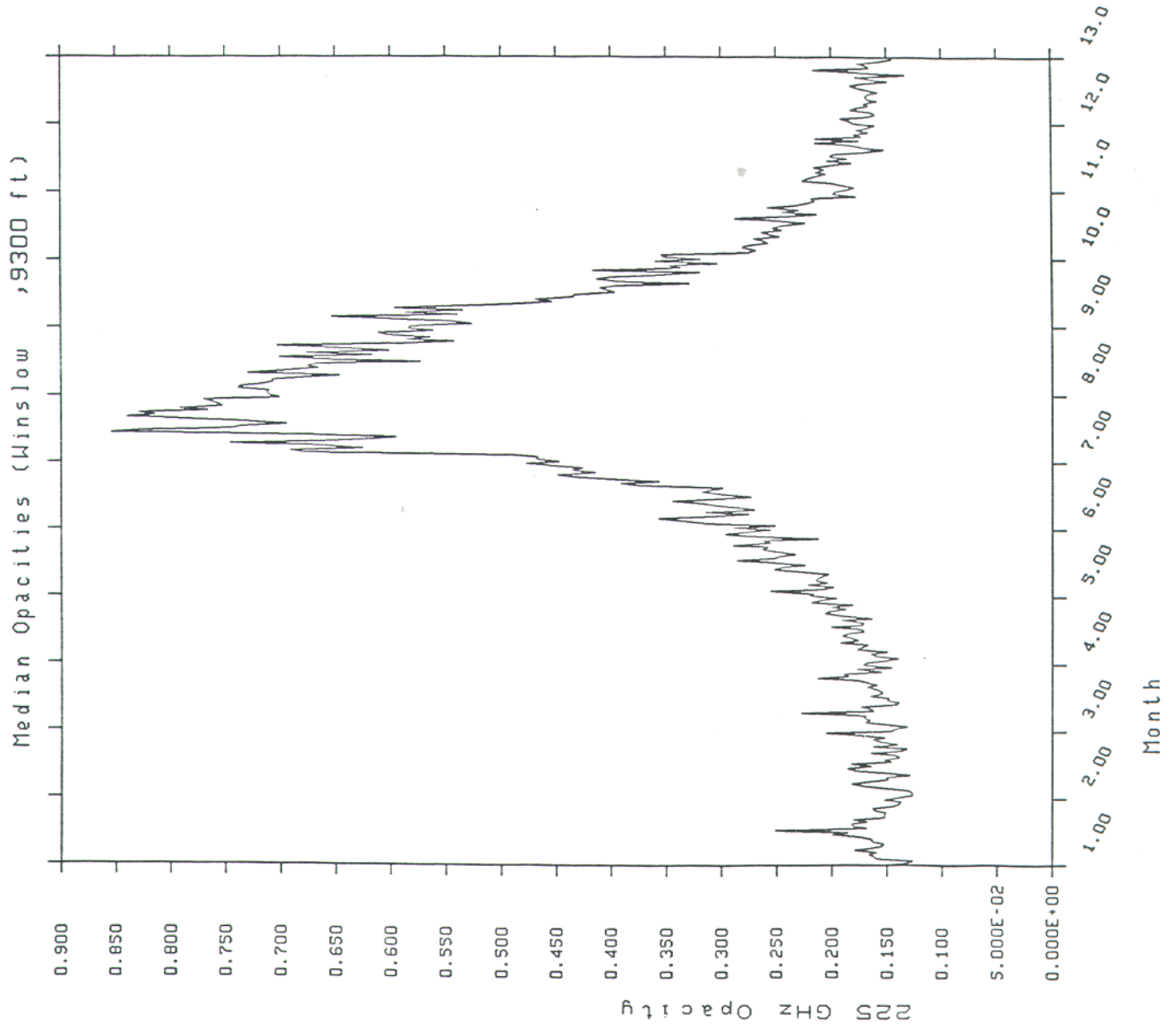


Fig. 23

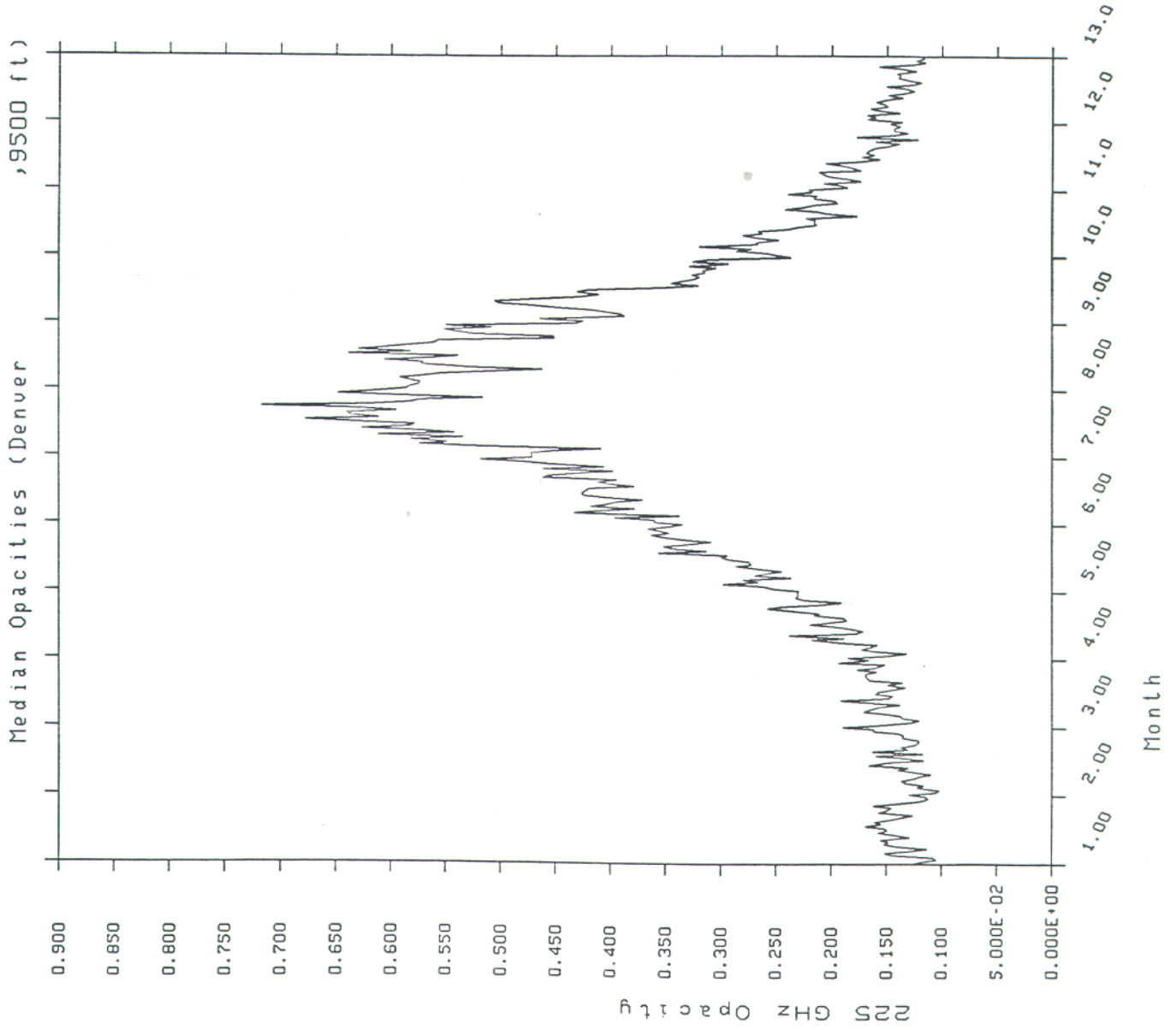


Fig. 24

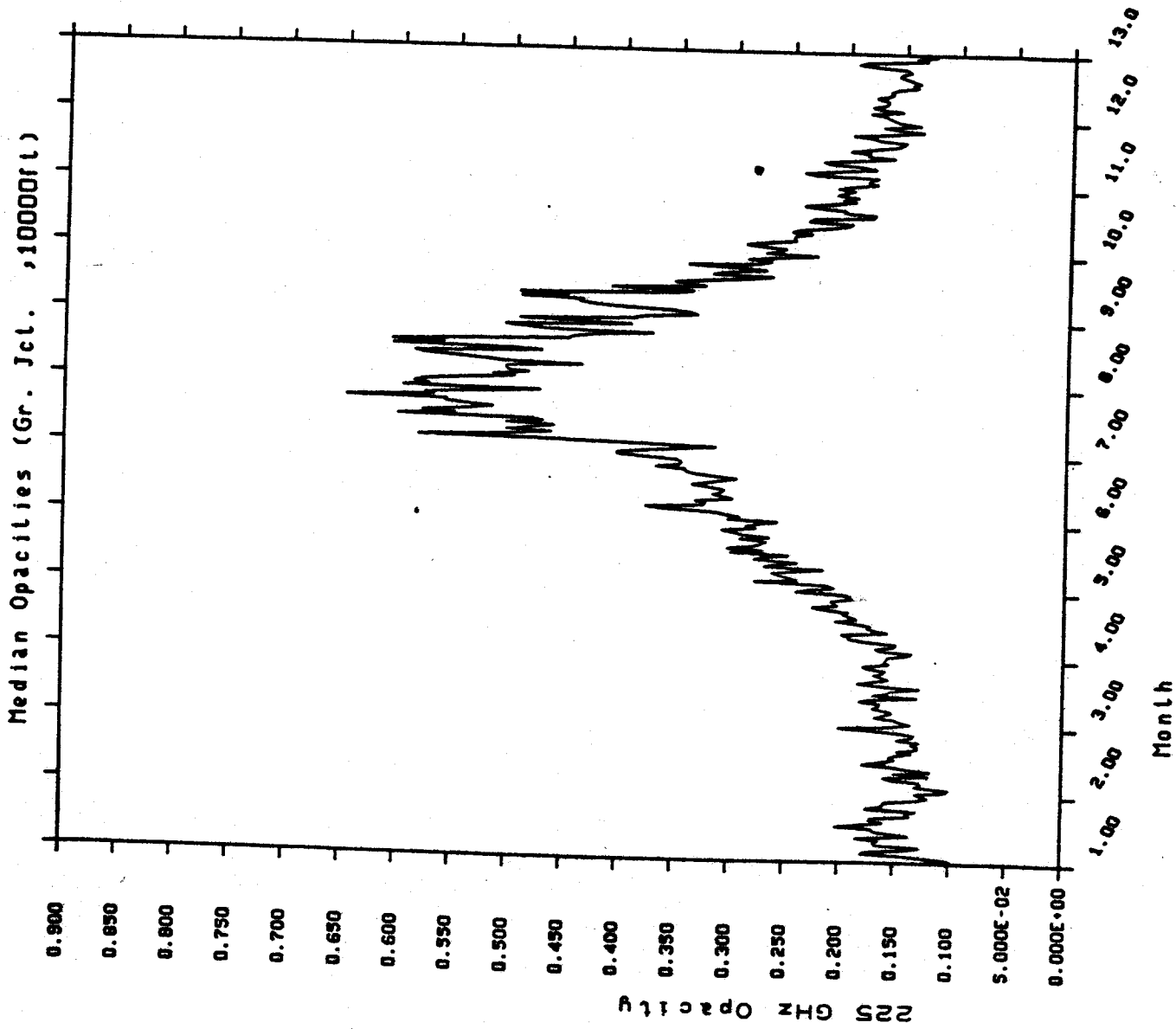


Fig. 25

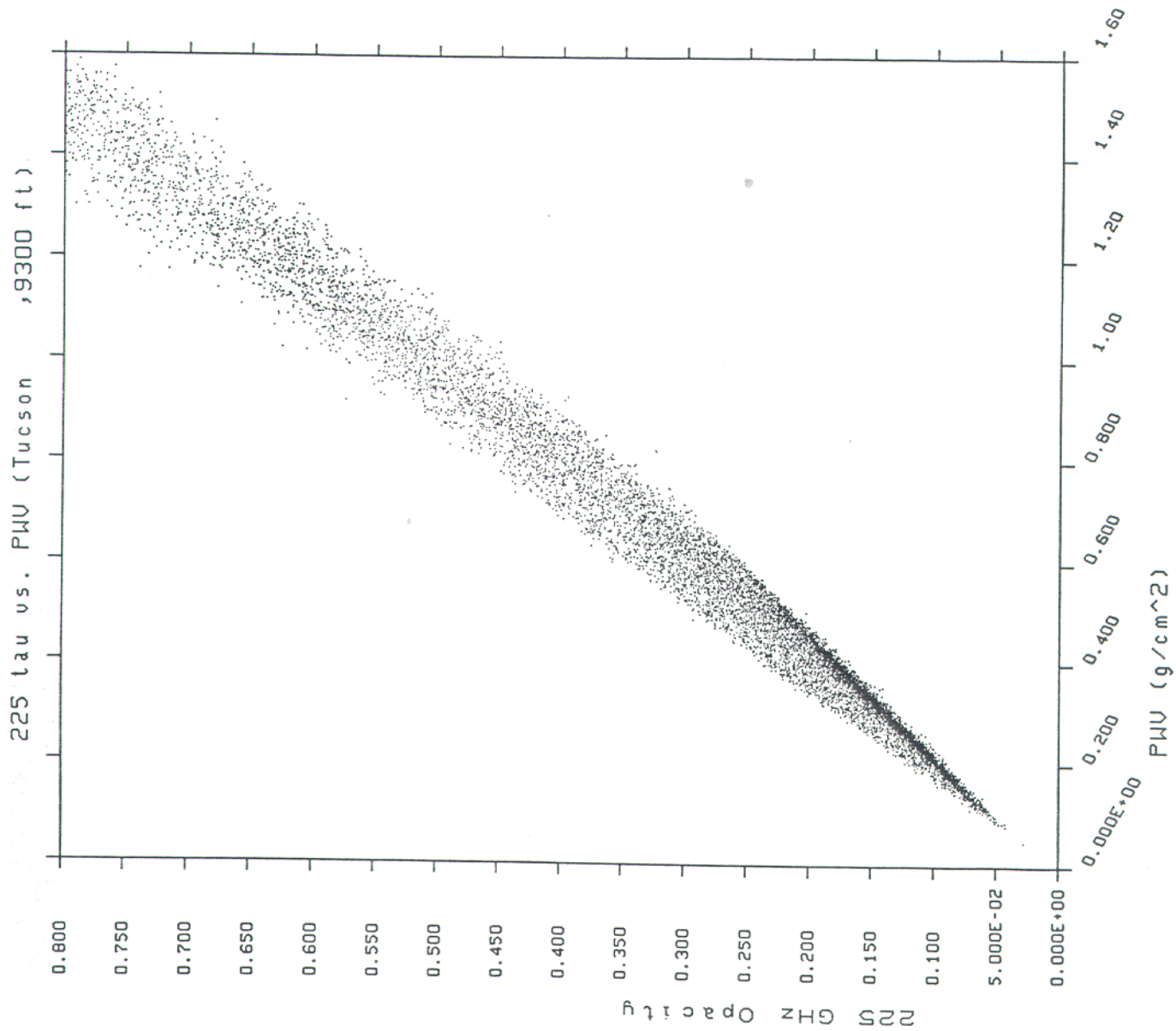


Fig. 26

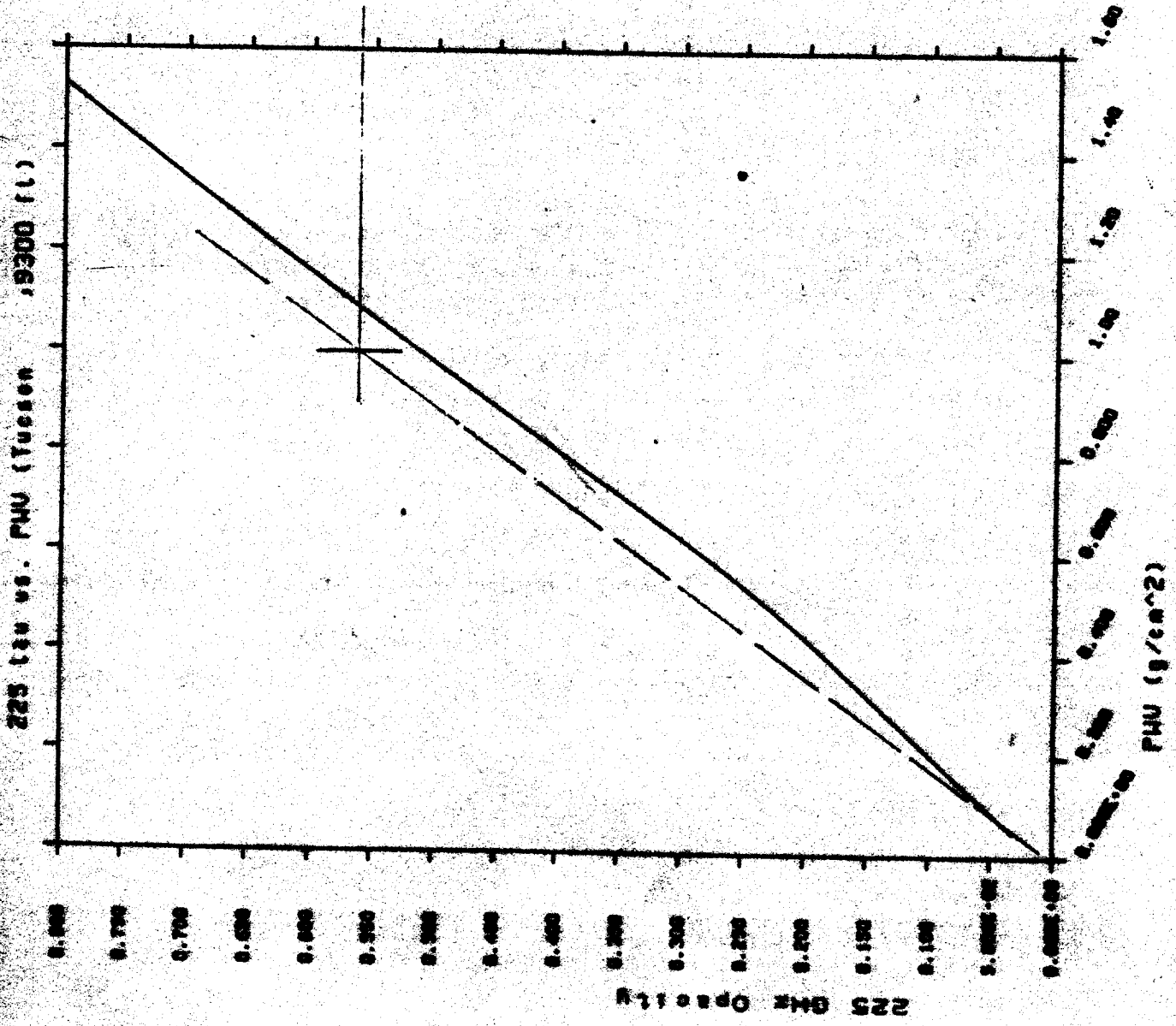


Fig. 27

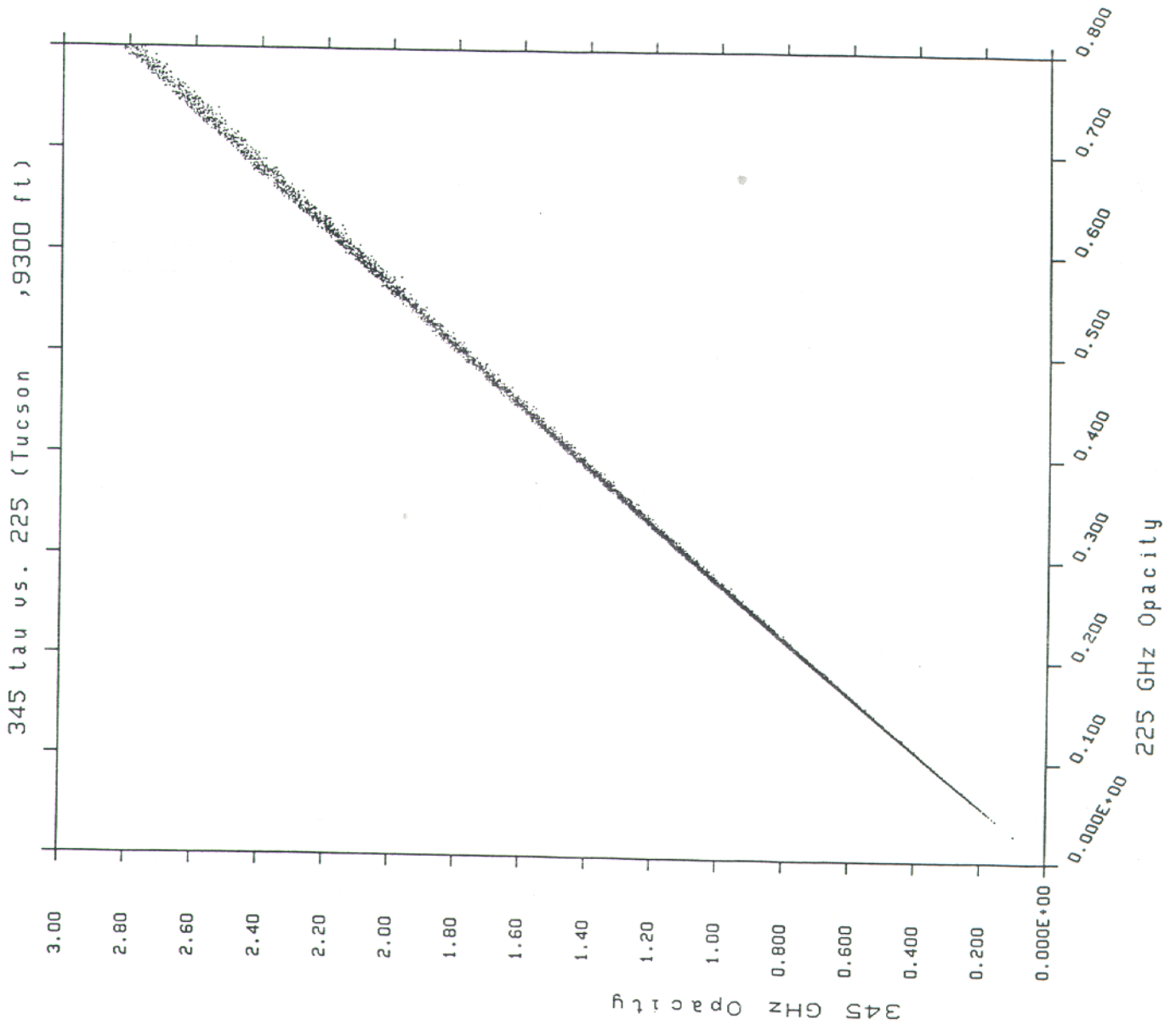


Fig. 28

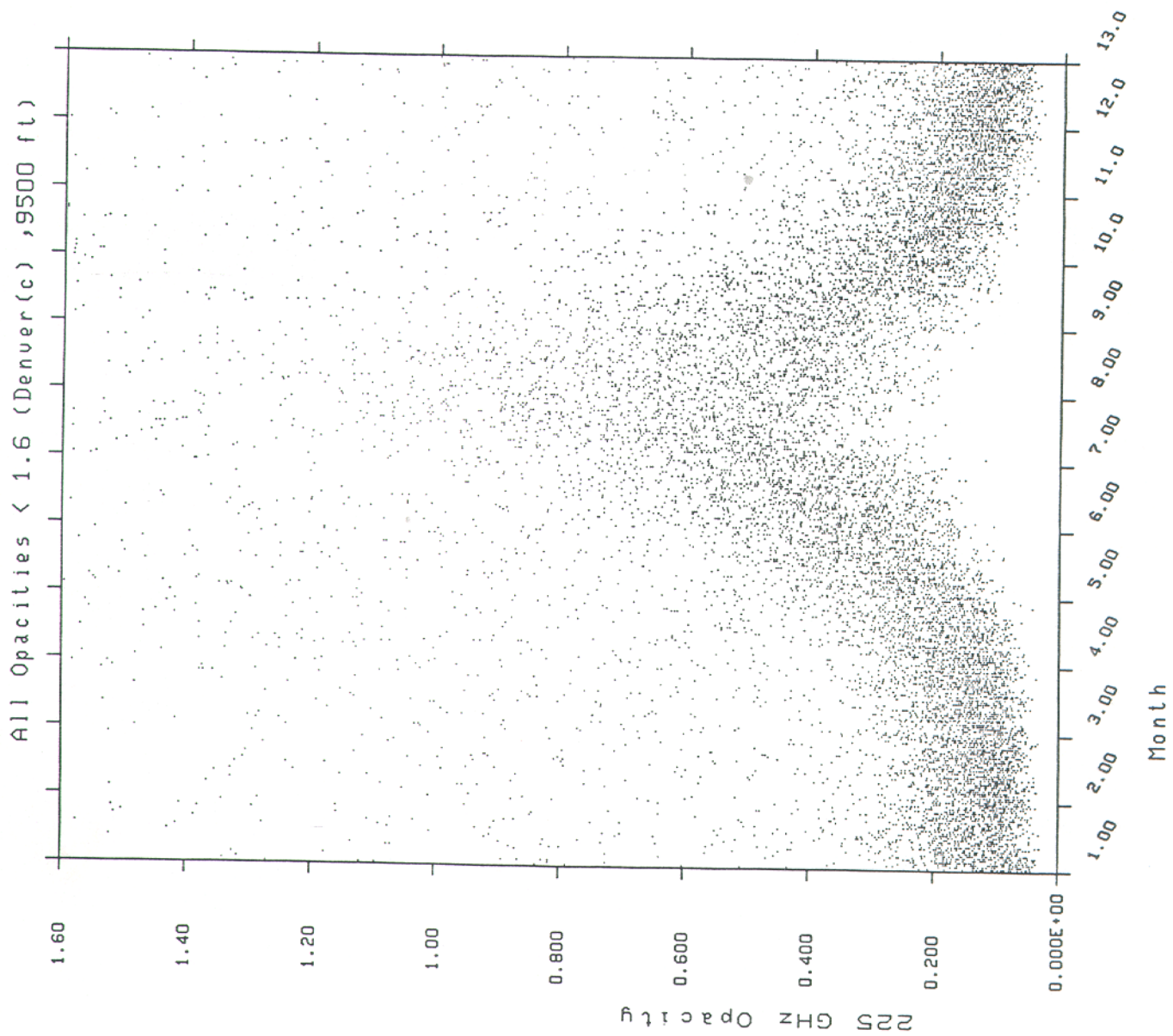


Fig. 29

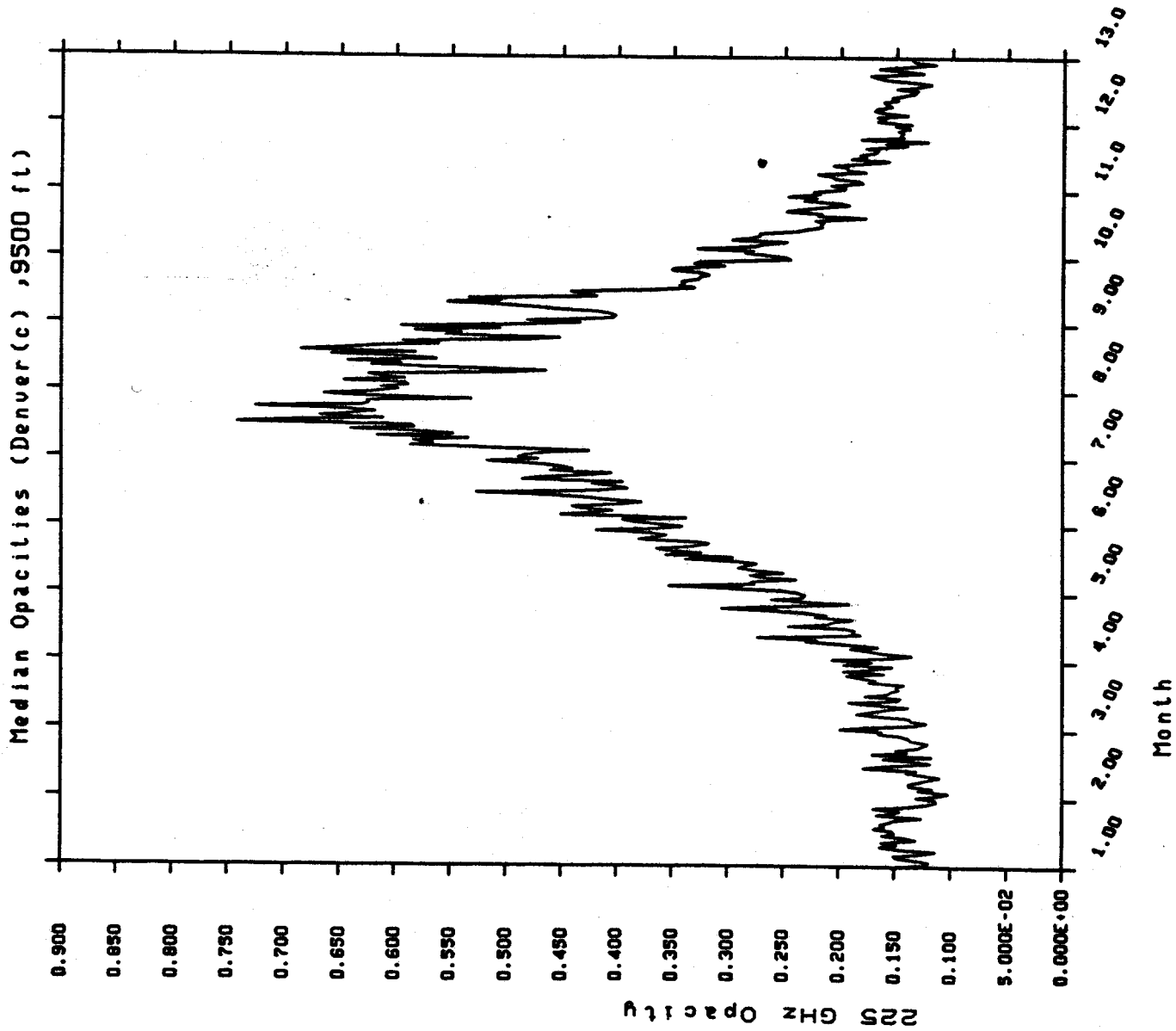


Fig. 30

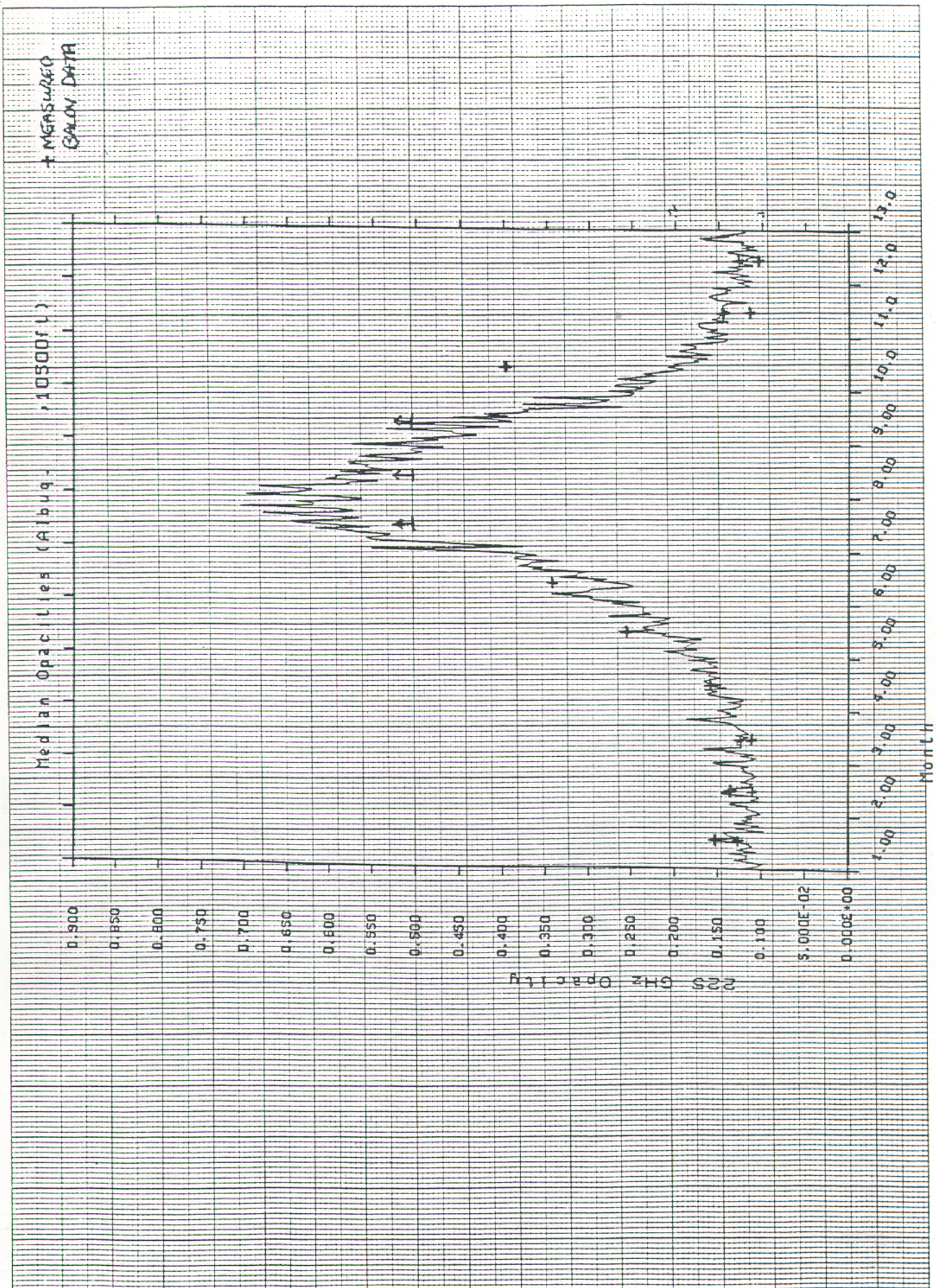


Fig. 31